Plant Biotechnology 33, 1–9 (2016)
DOI: 10.5511/plantbiotechnology.15.1117a

Original Paper

An MYB transcription factor regulating specialized metabolisms in *Ophiorrhiza pumila*

Emelda Rosseleena Rohani[1], Motoaki Chiba[1], Miki Kawaharada[1], Takashi Asano[1,a], Yoshimi Oshima[3], Nobutaka Mitsuda[3], Masaru Ohme-Takagi[3,4], Atsushi Fukushima[2], Amit Rai[1], Kazuki Saito[1,2], Mami Yamazaki[1,*]

[1] Graduate School of Pharmaceutical Sciences, Chiba University, Chiba 260-8675, Japan; [2] RIKEN Center for Sustainable Resource Science, Kanagawa 230-0045, Japan; [3] Bioproduction Research Institute, AIST, Tsukuba, Ibaraki 305-8566, Japan; [4] Graduate School of Science and Engineering, Saitama University, Saitama 338-8570, Japan
* E-mail: mamiy@faculty.chiba-u.jp Tel & Fax: +81-43-226-2932

Received October 5, 2015; accepted November 17, 2015 (Edited by T. Aoki)

Abstract Camptothecin is a plant-derived alkaloid and important precursor of clinically used anti-tumor drugs, but little is known about regulatory mechanism of camptothecin production in plants. We show here that a MYB transcription factor, *Op*MYB1, isolated from *Ophiorrhiza pumila* is a regulator of camptothecin biosynthesis. *Op*MYB1 has an EAR-like motif and exhibits a transcriptional repression activity in an in vivo assay using *Arabidopsis thaliana* leaves. Overexpression of *OpMYB1* in hairy roots of *O. pumila* resulted in reduced production of camptothecin and reduced expression of *OpTDC* encoding triptophane decarboxylase catalyzing the earliest step in camptothecin biosynthesis. From the deep transcriptome analysis, GO enrichment in secondary (specialized) metabolisms, especially in phenylpropanoid pathway was observed in the hairy roots over-expressing *OpMYB1*. Furthuremore, gene suppression by OpMYB1 was revealed in biosynthetic pathways of seco-iridoids, monoterpene indole alkaloids, anthraquinone and chlorogenic acid. These results suggested that *Op*MYB1 is a negative regulator to fine-tune the general specialized metabolisms in *O. pumila*.

Key words: Camptothecin, EAR-like motif, *Ophiorrhiza pumila*, repressor, R2R3-MYB.

Camptothecin, a plant derived monoterpene indole alkaloid (MIA), has been received attention for its anti-tumor activity due to strong inhibitory action upon DNA topoisomerase I (Hsiang et al. 1985; Redinbo et al. 1998). Camptothecin was firstly isolated from *Camptotheca acuminata* by Wall et al. (1966). The therapeutic values of camptothecin has been reported against colon cancer (Giovanella et al. 1989), lung cancer (Beretta et al. 2006), falciparum malaria (Bodley et al. 1998), and protozoan *Leishmania donovani* (Werbovetz et al. 2000). Nowadays, water-soluble semi-synthetic derivatives of camptothecin, e.g. irinotecan (Wiseman and Markham 1996) and topotecan (Ahmad and Gore 2004), are used clinically to treat colorectal and ovarian cancer respectively. On the contrary to the huge demand of camptothecin in pharmaceutical market, the supply is depend on plant resources, such as cultivated trees of *Camptotheca acuminate* (Vincent et al. 1997) and *Nothapodytes foetida* (Govindachari and Viswanathan 1972). Searching the alternative stable sources, various trials have been made on in vitro production of camptothecin in cell culture. However, the productivity of camptothecin by cell culture have been quite low (less than 0.005% dry weight) even with various improvements, for example, illumination with modified wave length on callus culture *of C. acuminata* (Park et al. 2003) or modification of nitrogen source on *Nothapodytes nimmoniana* (Karwasara and Dixit 2012). Hairy root culture of *Ophiorrhiza pumila* gave feasibility on camptothecin production in vitro at the level of ca. 0.1% dry weight (Saito et al. 2001) and it was applied to a bioreactor system (Sudo et al. 2002). Furthermore, ectopic expression of *ORCA3*, a regulatory gene of MIA biosynthesis from *Catharunthus roseus* (Van der Fits and Memelink 2001) enhanced camptothecin production in hairy roots of *C. acuminata* (Ni et al. 2011).

Camptothecin biosynthesis pathway is derived from strictosidine, a common intermediate of MIA

Abbreviations: CSC, cell suspension culture; HR, hairy root; MYBox, *OpMYB1* overexpressing hairy roots; MIA, monoterpene indole alkaloid; TDC, tryptophan decarboxylase; SLS, secologanin synthase; G10H, geraniol-10-hydroxylase; STR, strictosidine synthase; EAR, ERF-associated amphiphilic repression.

[a] Present address: School of Pharmacy, Iwate Medical University, Iwate 028-3694, Japan

This article can be found at http://www.jspcmb.jp/
Published online February 13, 2016

Table 1. EAR motif containing R2R3-MYB repressors in plants.

Protein Name	AGI Code/Accession No	Plant Species	Core EAR motif	Target Phenotype	References
OpMYB1	LC076107	*Ophiorrhiza pumila*	VNLEL		This study
AtMYB3	AT1G22640	*Arabidopsis thaliana*	LNLEL		Kagale et al. (2010)
AtMYB7	AT2G16720		LNLEL	phenyl propanoid and flavonoid pathway [a]	Wang and Dixon (2012)
AS1	AT2G37630		LELQL	leaf morphology [b]	Machida et al. (2015)
AtMYB32	AT4G34990		LDLNLEL	phenylpropanoid biosynthesis [a,b]	Preston et al. (2004)
AtMYB4	AT4G38620		LNLEL	phenylpropanoid biosynthesis [a,b]	Jin et al. (2000)
FaMYB1	AAK84064	*Fragaria×ananassa*	LNLDL	anthocyanin and flavonol [b]	Aharoni et al. (2001)
AmMYB330	P81395	*Antirrhinum majus*	VDLEL	phenylpropanoid and lignin biosynthesis [b]	Tamagnone et al. (1998)
MtMYB2	ABR28329.1	*Medicago truncatula*	LNLDL	proanthocyanidin and anthocyanin biosynthesis[b]	Jun et al. (2015)

[a] validated as transcriptional repressors; [b] supported by molecular genetic evidence as negative regulators.

biosynthesis. Strictosidine is produced by condensation of tryptamine and secologanin catalyzed by strictosidine synthase (STR) (Kutchan 1995). Strictosidine is then converted to strictosamide by intramolecular cyclization (Hutchinson et al. 1979). However, the steps following strictosamide to camptothecin biosynthesis have not been clearly defined. The plausible intermediates, pumiloside, 3(*S*)- and 3(*R*)-deoxypumiloside, were reported in *Ophiorrhiza pumila* (Aimi et al. 1989; Kitajima et al. 1997). However, the regulatory mechanism in camptothecin producing species is still unclear. So far, our research group has investigated on the detail of camptothecin production in hairy roots of *O. pumila* (Rubiaceae). Gene suppression of two catalytic enzymes in the early steps of MIA biosynthesis, tryptophan decarboxylase (TDC) and secologanin synthase (SLS), resulted in reduced accumulation of camptothecin and related alkaloids. From the non-targeted metabolite profiling of these suppressed hairy roots, candidates for biosynthetic intermediates were predicted (Asano et al. 2013). While the hairy roots of *O. pumila* are rich in specialized metabolites not only camptothecin-related alkaloids but also anthraquinones, de-differentiated cell suspension culture derived from hairy roots accumulated no alkaloids and faint amount of anthraquinones (Asano et al. 2013). The deep transcriptome analysis coupled with untargeted metabolic profiling between hairy roots and cell suspension culture showed differential expression of genes involved in the biosynthetic pathways of camptothecin, anthraquinones and chlorogenic acid (Yamazaki et al. 2013).

In this study, a gene encoding R2R3-myb transcription factor, *OpMYB1*, was isolated as one of hairy root specific genes which is not expressed in cell suspension culture. *Op*MYB1 contains an EAR-like motif known to be repression domain (Table 1). For the functional characterization, *OpMYB1* was overexpressed in hairy roots and alkaloid production and transcriptome change in them were analyzed. This is the first report of a regulator concerning on the camptothecin biosynthesis in *O. pumila*.

Materials and methods

Plant materials and tissue cultures

Hairy roots were induced from stem segments of in vitro plant culture of *O. pumila* as described by (Saito et al. 2001). Cell suspension culture was induced from the hairy roots as reported (Asano et al. 2013).

Isolation and sequence analysis of OpMYB1

Differentially expressed genes between hairy roots and cell suspension culture were profiled by PCR-select cDNA subtraction and fragmental sequences were obtained (Clontech, Japan) as described by Bunsupa et al. (2011). Based on the sequence information of the fragment showing homology with myb transcription factors, a full-length cDNA was cloned by performing 5′- and 3′-RACE.

Homologous genes were searched using the BLASTx program against Non-redundant (nr) protein sequence and UniProtKB/SwissProt (swissprot).

A phylogenetic tree was constructed using the neighbor-joining method of MEGA6 (Tamura et al. 2013). Bootstrap values were statistically calculated with the default setting of the MEGA6 program. Amino acid sequence alignment was performed between *OpMYB1* with five-selected MYB from the same clade from the phylogenetic analysis, and *Arabidopsis thaliana* MYB using CLC Main Workbench 7 software (CLC Bio, Qiagen).

Transient effector-reporter assay

An open reading frame of *OpMYB1* was amplified by PCR and subcloned into 35S:GAL4DB vector pDEST430T1.2 (Ohta et al. 2000) using Gateway technology (Invitrogen). The reporter construct, Pro35S-GAL4-TATA-LUC-HSP (Tanaka et al. 2012), contains the five repeats of GAL4 binding site fused CaMV35S minimal promoter, a luciferase gene and transcriptional terminator of a heat shock protein 18.2 gene. The primers used were OpMYB1-ORF-attB1-F and OpMYB1-ORF-attB2-R (Supplementary Table S1). The empty vector pDEST430T1.2

without insertion (35S:GAL4DB) was used as negative control. Effector and reporter plasmids were co-bombarded into the leaves of *Arabidopsis thaliana* grown in long-day condition (16-h-light/8-h-dark cycle).

Construction of binary vectors and plant transformation

Stable transformed hairy roots over-expressing *OpMYB1* (MYBox) were obtained as follows. The open reading frame of *OpMYB1* was subcloned into the binary expression vector pH7WG2D (Nakagawa et al. 2007) through Gateway technology (Invitrogen, USA) and pH7WG2D-*OpMYB1* ($35S_{pro}$:*OpMYB1*) was obtained. For negative control, *GUS* (β-glucuronidase) gene was used instead of *OpMYB1*. The binary vector pH7WG2D-*OpMYB1* or pH7WG2D-*GUS* was introduced into *Agrobacterium rhizogenes* (pRi15834) by electroporation. The stem sections of *O. pumila* were co-cultured with *A. rhizogenes* harboring the binary vector and transgenic hairy roots transformed with T-DNA from binary vectors were obtained as described previously by Asano et al. (2009).

Gene expression analysis of MYB-overexpressing lines by RT-PCR

Total RNA was extracted from MYBox and GUS lines using RNeasy plant mini kit (Qiagen) and treated with DNase. Subsequently, each sample of total RNA (1 μg) was subjected to reverse transcription using SuperScript II Reverse Transcriptase kit (Invitrogen) using Oligo dT-3 sites Adaptor Primer (TaKaRa).

The semi-quantitative RT-PCR analysis was performed on *OpMYB1* using primer set of OpMYB1-F and OpMYB1-R (Supplementary Table S2). The expression of housekeeping β-tubulin gene was analyzed as a control with primer set of OpTub-F and OpTub-R. PCR amplification was performed with denaturation step at 94°C for 1 min 30 s, followed by 26 cycles at 94°C for 30 s, 55°C for 30 s, and 72°C for 2 min 30 s. The PCR products were separated by electrophoresis using 1.5% agarose gel. The gel was then stained with SYBR Green I nucleic acid gel stain (Invitrogen) and afterwards scanned with Storm 860 image analyzer (GE Healthcare). The produced image scan were visualized and analyzed using Image Quant (GE Healthcare). The expression level of *OpMYB1* was calculated by normalization with β-tubulin band and later compared to the average value of GUS-expression level.

RT-PCR based quantification of key enzyme coding genes in MIA biosynthesis pathway was performed using primersets, OpTDC-F and OpTDR-R, OpG10H-F and OpG10H-R, OpSLS-F and OpSLS-R, and OpSTR-F and OpSTR-R (Supplementary Table S2) with the same PCR condition as described above.

Analysis of camptothecin

Camptothecin contents in the MYBox samples from 3-weeks culture were extracted and quantified by HPLC equipped with fluorescent detector as described previously by Asano et al. (2013).

Deep transcriptome sequencing, de novo assembly and annotation

Deep transcriptome analysis was performed as described previously (Yamazaki et al. 2013). Poly(A)+ RNA was isolated from 3-week-old MYBox. A cDNA library was constructed and sequenced using pair-end method with an Illumina platform (Riken Genesis). The Illumina reads were deposited in the DNA Data Bank of Japan (DDBJ) under Sequence Read Archive (DRA) with accession No. DRA000931, with experiment No. DRX003679 for HR and DRX003680 for MYBox. Previously, reads with accession No. DRA000930, with experiment No. DRX003677 for CSC and DRX003678 for HR were deposited by Yamazaki et al. (2013).

The generated raw reads were cleaned based on quality score and adaptors were removed, and assembled using Trinity program (Grabherr et al. 2011). The assembly procedure (including cleaning, alignment and abundance estimation) and annotation (including BLAST alignment, assigning EC number and functional classification) were done following Fukushima et al. (2015).

Results and discussion

Structure of OpMYB1

A differential PCR-select subtraction was performed using cDNAs from hairy roots and cell suspension culture. The 353 gene fragments that differentially expressed in hairy roots were sequenced. Nearly 40% of these fragments were annotated as metabolic enzymes and the rest were transporters, transcription factors and stress-related proteins (data not shown). Among hairy-root specific fragments, 15 fragments were annotated as transcription factors including a MYB transcription factor (Supplementary Table S3). Considering the general role of MYB transcription factors in the regulation of specialized metabolisms, we selected this fragment for further investigation. Based on the nucleotide sequence of the MYB fragment, a full-length cDNA was cloned by 5′- and 3′-RACE and designated as *OpMYB1*.

OpMYB1 encodes 304 amino acids the deduced from nucleotide sequence (registered as LC076107 in DDBJ/GenBank). *Op*MYB1 is classified into R2R3 type MYB, and has following conserved motifs; bHLH-interaction domain, GIDP motif, ERF-associated amphiphilic repression (EAR) -like motif (VNLDL) and zinc finger motif (Figure 1). The EAR motif (LxLxL or DLNxxP) was widely conserved in diverse transcriptional repressors (Kagale et al. 2010, 2011). R2R3-MYB containing EAR-motif containing are distributed across different plant species and some of them were identified as negative regulator of transcription (Table 1).

Phylogenetic tree was constructed using amino acid

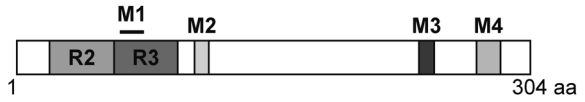

Figure 1. Schematic representation of protein domains in *Op*MYB1. R2 and R3, Repeat sequences conserved in R2R3 MYB transcription factors; M1, bHLH-interaction domain; M2, GIDP motif; M3, EAR-like motif; M4: Zinc finger motif.

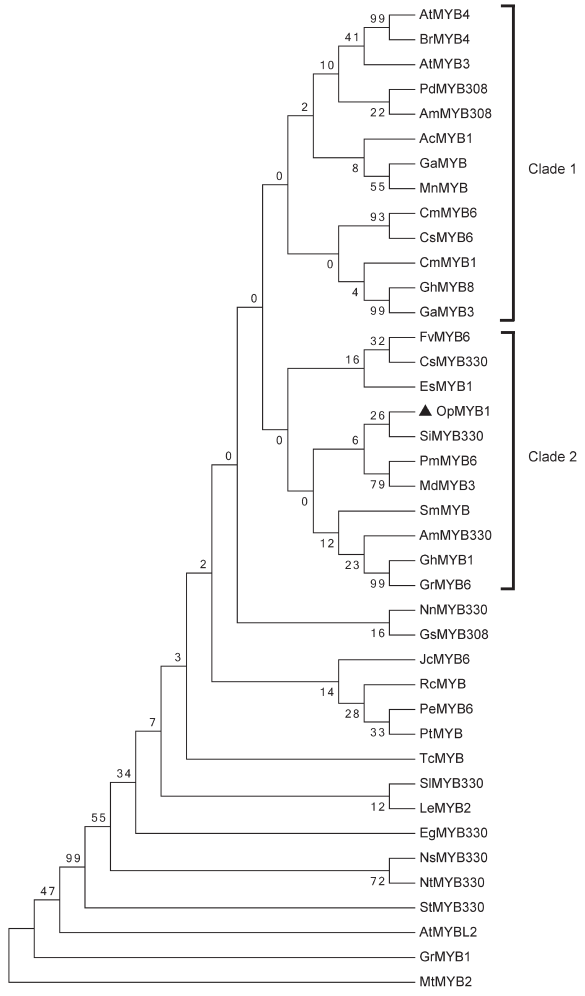

Figure 2. Phylogenetic tree of R2R3-MYBs containing EAR motif, based on predicted amino acid sequences. The number on the branches indicates the bootstrap support values (500 replicates). Accession numbers of the MYB sequences are listed in Supplementary Table S4.

sequences of *Op*MYB1 and R2R3-MYBs containing EAR-motif (Figure 2, Supplementary Table S4). *Am*MYB330 in the same Clade 2 as *Op*MYB1 has been identified as a negative regulator in phenylpropanoid and lignin biosynthesis in *Antirrhinum majus* (Tamagnone et al. 1998). *At*MYB4 belongs to Clade 1, which was next to *Op*MYB1's Clade 2, also being reported as a repressor of phenylpropanoid and lignin biosynthesis (Kranz et al. 1998). This suggests that *OpMYB1* is a potential negative regulator of specialized metabolism in *O. pumila*.

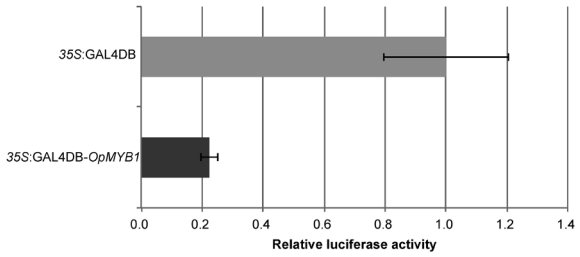

Figure 3. Transcriptional repressor activity of *Op*MYB1. Transient effector-reporter analysis was performed. The effector and the reporter constructs were co-transformed into the leaves of *Arabidopsis thaliana*. The reporter construct (35S-5xGAL4:LUC) contains the five repeats of GAL4 binding site fused CaMV35S minimal promoter and a luciferase gene. 35S:GAL4DB-OpMYB1, OpMYB1 fused to GAL4-binding domain was expressed under control of CaMV35S promoter. *35S*:GAL4DB, only GAL4-binding domain was expressed (negative control). LUC activity with negative control was set to 1. Each bar represents the mean±SE of six biological replicates. Statistical significance was observed by the Student's *t*-test, p-value <0.05.

Transcriptional repressor activity of OpMYB1

To examine the transcriptional activation/repression activity of *Op*MYB1, transient effector-reporter analysis was performed. The reporter construct (*35S*:5xGAL4BS-*LUC*) and the effecter construct (*35S*:GAL4BD-*OpMYB1*) were co-transformed by particle bombardment into leaves of *Arabidopsis thaliana*. The luciferase activity was reduced one fifth comparing with the negative control (35S:GAL4BD) with a significant difference ($p<0.05$) (Figure 3). This result supported the idea that *OpMYB1* acts as a negative transcriptional regulator in *O. pumila*.

OpMYB1 overexpression in transgenic hairy roots

In order to clarify the function of *OpMYB1*, the *OpMYB1* was overexpressed in hairy roots. The 17 lines of hairy roots were successfully obtained. The expression of *OpMYB1* in transformed hairy roots was determined by semi-quantitative PCR (Supplementary Figure S1). The expression levels of *OpMYB1* in *OpMYB1*-overexpressing hairy roots (MYBox) were compared with those in the control hairy roots transformed with β-glucuronadase gene (GUS). The five lines had increased OpMYB1 expression level more than 4 fold and the highest expression was 5.2-fold compared to the average value of control lines. The well growing ten MYBox lines were selected for further investigation and numbered (1–10) according to their expression level of *Op*MYB1.

Subsequently, camptothecin accumulation in MYBox was compared with control hairy roots (Figure 4). The methanol extract of individual hairy root lines were subjected to HPLC analysis monitored fluorescent detector. A negative correlation was observed between the content of camptothecin and the expression level of *OpMYB1*. This result suggests that OpMYB1 has a role of negative regulator in camptothecin biosynthesis. Then,

the expression levels of several genes encoding catalytic enzymes in early steps in MIA biosynthesis (Yamazaki et al. 2003) were determined. The expression levels of *OpTDC*, *OpG10H*, *OpSLS* and *OpSTR*, that encoding tryptophane decarboxylase, geraniol 10-hydroxylase, secologanin synthase and strictosidine synthase respectively, were determined by semi-quantitive RT-PCR (Figure 5). The expression level of *OpTDC* showed a significant negative correlation ($r=-0.701$, $p<0.01$) with that of *OpMYB1*. This result showed that *Op*MYB1 inhibits the expression of *OpTDC* at least. However, the effects on other enzyme genes were not clear. The knockdown of *OpMYB1* by RNAi showed no significant change both in camptothecin production and gene expression of catalytic enzymes (data not shown).

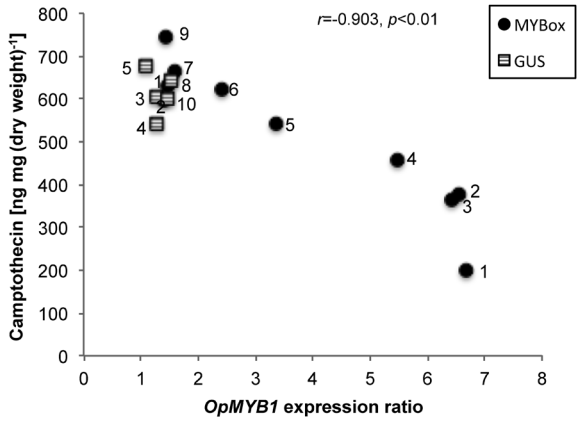

Figure 4. Relative expression levels of *OpMYB1* and camptothecin contents in MYBox and GUS lines. The expression of *OpMYB1* was measured by semi-quantitative RT-PCR normalized by the expression level of *β*-tubulin gene. The expression ratio was calculated to the average of in GUS control lines as 1. The numbers on each point means line number of biological replicate ($n=3$). Statistical significance was observed by Pearson correlation coefficient and Student's *t*-test, at $r=-0.903$ and $p<0.01$, respectively.

De novo transcriptome assembly and functional annotation

Total RNA prepared from MYBox was subjected to deep transcriptome analysis. The 2 Gb of paired-end reads were generated and analyzed together with those previously obtained by Yamazaki et al. (2013) from cell suspension culture (CSC) and hairy roots (HR) (Table 2). Finally, the total contigs of 59,855 were retrieved from de novo assembly with an average length of 989 bp (Table 3).

The Blast2GO program v 2.7.1 (Conesa et al. 2005) was used to identify differentially enriched Gene Ontologies by Fisher's exact test with threshold set at 0.05. Differentially expressed unigenes in MYBox compared to HR were used as test set against annotated transcriptome of *O. pumila*, resulting in 57 GO categories enriched due

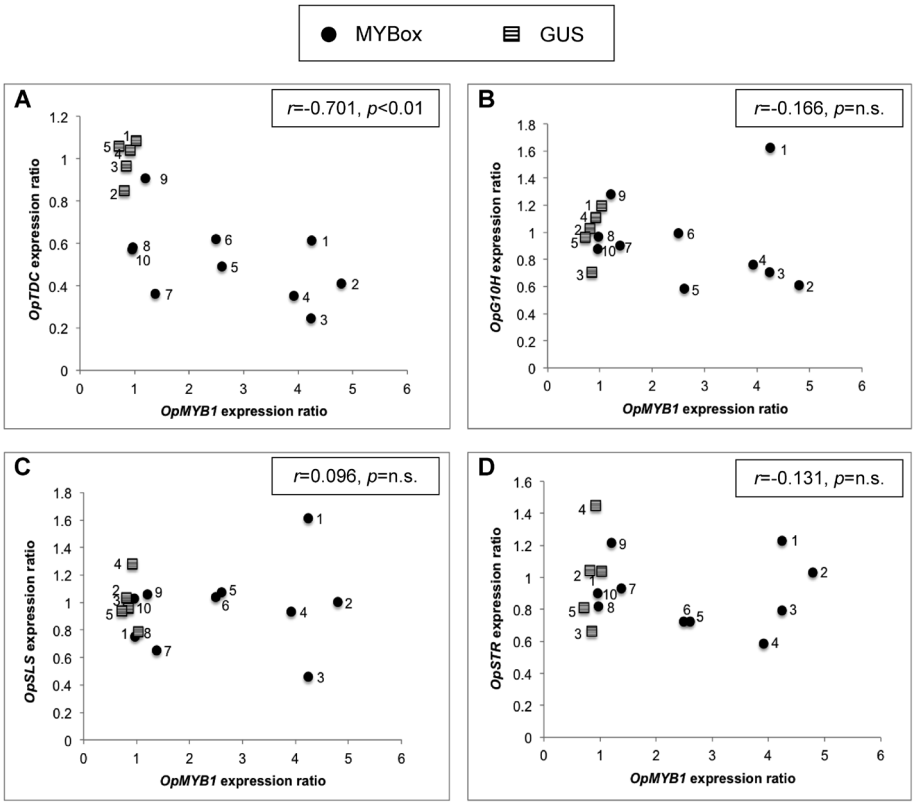

Figure 5. Relative expression level of *OpMYB1* and transcript levels of enzyme genes in camptothecin biosynthetic pathway in MYBox and *GUS* lines. (A) *OpTDC* (B) *OpG10H*, (C) *OpSLS* (D) *OpSTR* In each graph, The numbers on each point means line number with biological replicate ($n=3$). The *r* and *p* values were obtained by Pearson correlation coefficient and Student's *t*-test, respectively.

to *OpMYB1* overexpression. Among these, GO terms corresponding to secondary (specialized) metabolite biosynthesis process, including phenylpropanoids were among top ten enriched GO terms in our test set (Figure 6, Supplementary Table S5). This result consistent with the fact that *At*MYB4, *At*MYB7, *At*MYB32 and *Am*MYB330 play roles as negative regulators in phenylpropanoid biosynthesis in *Arabidopsis thaliana* and *Antirrhinum majus* respectively (Nakano et al. 2015; Tamagnone et al. 1998). Moreover, GO term corresponding to oxidation-reduction process was also enriched in MYBox. Many oxidation-reduction processes might be involved in specialized metabolisms. Our results show that *OpMYB1* overexpression affected on general specialized metabolisms including camptothecin biosynthesis in *O. pumila*.

OpMYB1 involvement in specialized metabolisms including camptothecin biosynthesis

The expressions of genes encoding catalytic enzymes involved in early steps of camptothecin biosynthesis, *OpTDC*, *OpG10H*, *OpSLS* and *OpSTR*, (Yamazaki et al. 2003) were investigated with the transcriptome data assembly in this study. Contigs corresponding *OpTDC*, *OpG10H*, *OpSLS* and *OpSTR* were expressed at lower level in MYBox comparing to hairy roots (HR) although at still higher level than cell suspension culture (CSC) (Figure 7; Supplementary Figure S2). These results suggest that *Op*MYB1 transcription factor plays a role as negative regulator in early steps of MIA biosynthesis. As described above, the repression effect of *Op*MYB1 on *OpG10H*, *OpSLS* and *OpSTR* was not clear when the gene expression was quantified by semi-quantitive RT-PCR. Deep transcriptome analysis gave rather definite results than RT-PCR.

Seco-iridoid pathway reaches to secologanin production is the upstream process of MIA biosynthesis. Based on the information about *sec*-iridoid pathway genes in *Catharanthus roseus* producing vinca alkaloids (Miettinen et al. (2014), total of 81 contigs presumably involved in seco-iridoid pathway were predicted and their expression levels in MYBox were compared with those of in HR and CSC (Figure 7, Supplementary Figure S3). There is a general trend that the expression of genes in this pathway of MYBox was also reduced compared with that in HR.

Previously, the accumulation of anthraquinones has been reported in hairy roots and callus culture of *O. pumila* (Kitajima et al. 1998). They are a major group of specialized metabolites in Rubiaceae family. Anthraquinones in Rubiaceae have been reported to be synthesized by a formation of 1,4-dihydroxy-2-naphthoyl-CoA from chorismate pathway, with dimethylallyl diphosphate from MEP pathway (Han et al. 2001). For both chorismate and MEP pathways, contigs presumed to encode catalytic enzymes in anthraquinone pathway were extracted and their expression level

Table 2. Summary of RNA-seq analysis.

Items	Numbers
Total number of reads	80,065,066
Total reads of CSC	24,617,708
Total reads of HR	29,682,050
Total reads of MYBox	25,765,308
Average length of reads (bp)	90

CSC, cell suspension culture; HR, hairy roots; MYBox, *OpMYB1* overexpressing hairy roots.

Table 3. Summary of Trinity assembly.

Items	Numbers
Total assembled contigs	59,855
Maximum contig length (bp)	15,617
Minimum contig length (bp)	201
Average contig length (bp)	989
N75; N50; N25 (bp)	790; 1,722; 2,862

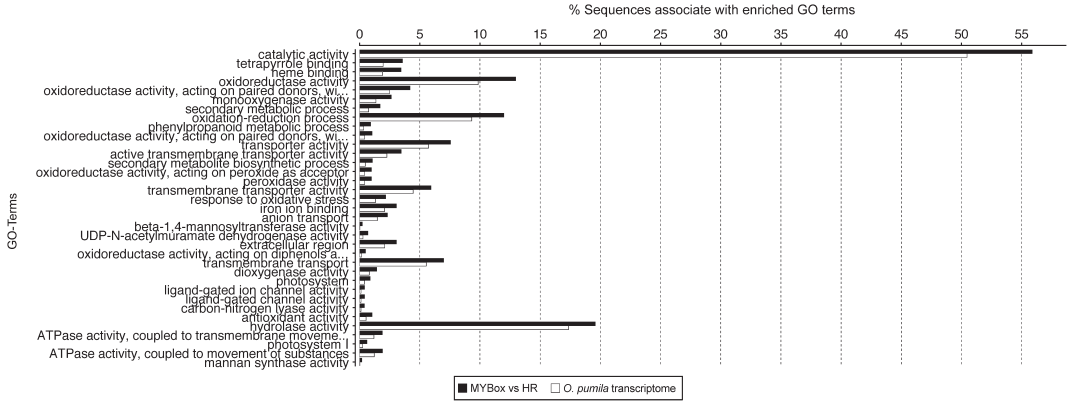

Figure 6. Differential GO enrichment for MYBox in *O. pumila*. Differentially expressed unigenes for MYBox with respect to hairy roots (MYBox vs HR) compared to *O. pumila* transcriptome dataset. Annotation from top to bottom is in the order of ascending *p*-value. Differential enrichment of GO terms were performed using Fisher's exact test with a *p*-value cutoff <0.05 applied.

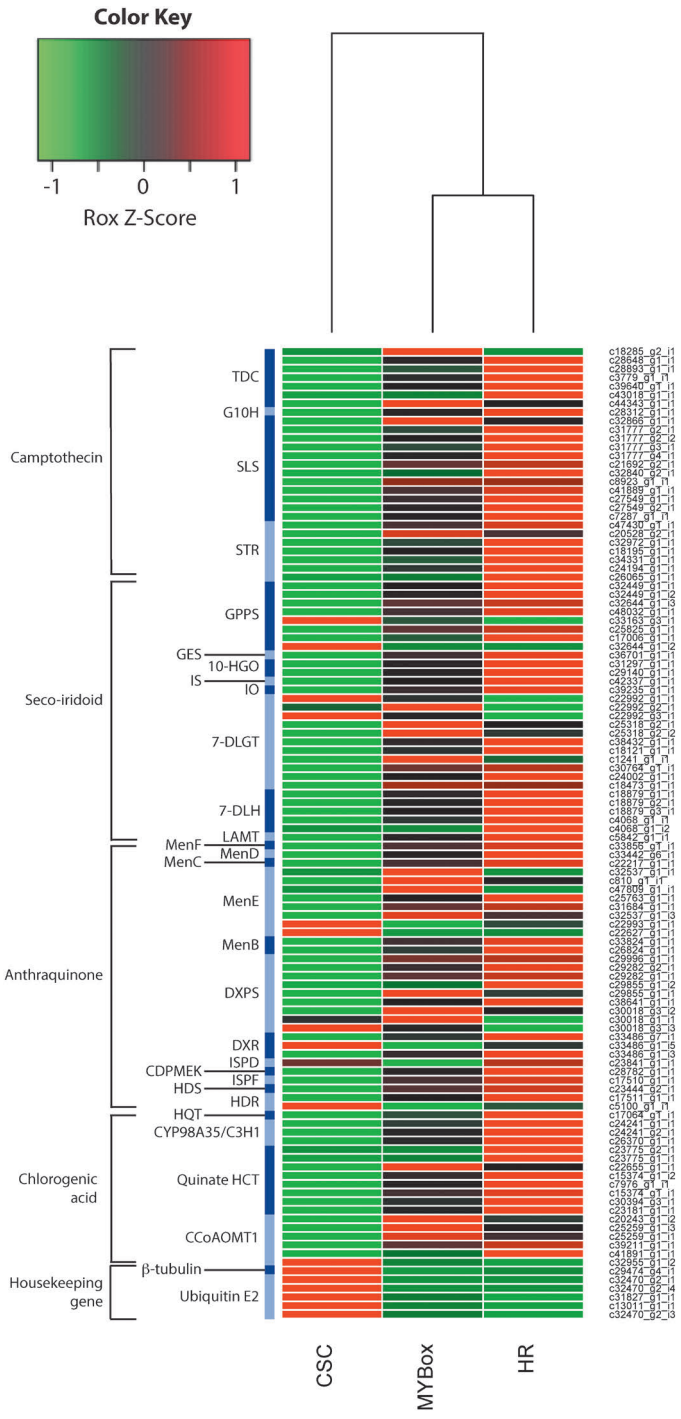

Figure 7. Heatmap diagram of expression level of genes involved in specialized metabolisms. Heat map was constructed according to FPKM value of genes involved in biosynthetic pathway of strictosidine, seco-iridoid, anthraquinone and chlorogenic acid, and housekeeping genes. The numbers on the right hand side are the contig ID. The expression levels are showed in red-green color scale. CSC, cell suspension culture; HR, hairy roots; MYBox, *OpMYB1*-overexpression in hairy roots; TDC, tryptophan decarboxylase; G10H, geraniol 10-hydroxylase; SLS, secologanin synthase; STR, strictosidine synthase; GPPS, geranyl diphosphate synthase; GES, geraniol synthase; 10-HGO, 10-hydroxygeraniol dehydrogenase; IS, iridoid synthase; IO, iridoid oxidase; 7-DLGT, 7-deoxyloganetic acid glucosyl transferase; 7-DLH, 7-deoxyloganic acid hydroxylase; LAMT, loganic acid *O*-methyltransferase; MenF; menaquinone-specific isochorismate synthase; MenD, 2-succinyl-5-enolpyruvyl-6-hydroxy-3-cyclohexene-1-carboxylate synthase; MenC, *o*-succinyl benzoate synthase; MenE, *o*-succinyl benzoic acid-CoA ligase; MenB, naphthoate synthase; DXPS, 1-deoxy-D-xylulose-5-phosphate synthase; DXR, 1-deoxy-D-xylulose 5-phosphate reductoisomerase; ISPD, 2-*C*-methyl-D-erythritol 4-phosphate cytidylyltransferase; CDPMEK, 4-diphosphocytidyl-2-*C*-methyl-D-erythritol kinase; ISPF, 2-*C*-methyl-D-erythritol 2,4-cyclodiphosphate synthase; HDS, (*E*)-4-hydroxy-3-methylbut-2-enyl diphosphate synthase; HDR, 4-hydroxy-3-methylbut-2-enyl diphosphate reductase; HQT, hydroxycinnamoyl-CoA quinate hydroxycinnamoyl transferase; CYP98A35 or C3H1, *p*-coumaroyl quinate/shikimate 3′-hydroxylase; Quinate HCT, caffeoyl-CoA:quinate *O*-(hydroxycinnamoyl) transferase; CCoAOMT1, caffeoyl-CoA 3-*O*-methyl transferase. Supporting information from BLAST search of contigs in this analysis are listed in Supplementary Table S6.

was displayed (Figure 7; Supplementary Figure S4) as reported by (Yamazaki et al. 2013). Again a general trend of reduced gene expression for this pathway in MYBox when compared with the expression in HR. Another specialized metabolism predicted in *O. pumila* is chlorogenic acid biosynthesis. The same trend of gene expression pattern, repressed in MYBox was observed on CYP98A35, C3H and quinate HCT (Figure 7; Supplementary Figure S5) as seen in other biosynthetic pathways.

On the other hand, no change was observed in the expression levels of housekeeping genes encoding β-tubulin and ubiquitin between MYBox and HR, while high expression in CSC with totally different expression pattern with those of genes involved in specialized metabolisms.

Taken together, this paper presented *Op*MYB1 as a key transcription factor that negatively regulates general specialized metabolisms in *O. pumila*, biosynthesis of seco-iridoid, MIA, anthraquinone and chlorogenic. So far, several studies have reported on repressor functions of R2R3-MYB containing EAR-motif on phenylpropanoid, lignin and flavonoid. Addition to zinc finger proteins with EAR-motif acting as transcriptional repressors of MIA biosynthesis genes in *Catharanthus roseus* (Pauw et al. 2004), it is the first report on R2R3-MYB suppresses alkaloid production. Using these information, candidate genes involved in camptothecin biosynthesis will be screened.

Acknowledgements

This research is funded by Grants-in-Aid for scientific research from the Ministry of Education, Culture, Sports, Science and Technology (MEXT) of Japan and The Japan Society for the Promotion of Science (JSPS) and CREST from Japan Science and Technology Agency (JST). We thank Prof. Tsuyosi Nakagawa for providing binary vector.

References

Ahmad T, Gore M (2004) Review of the use of topotecan in ovarian carcinoma. *Expert Opin Pharmacother* 5: 2333–2340

Aimi N, Nishimura M, Miwa A, Hoshino H, Sakai S, Haginiwa J (1989) Pumiloside and deoxypumiloside; plausible intermediates of camptothecin biosynthesis. *Tetrahedron Lett* 30: 4991–4994

Asano T, Kobayashi K, Kashihara E, Sudo H, Sasaki R, Iijima Y, Aoki K, Shibata D, Saito K, Yamazaki M (2013) Suppression of camptothecin biosynthetic genes results in metabolic modification of secondary products in hairy roots of *Ophiorrhiza pumila*. *Phytochemistry* 91: 128–139

Asano T, Sudo H, Yamazaki M, Saito K (2009) Camptothecin production by in vitro cultures and plant regeneration in *Ophiorrhiza* species. In: Jain SM, Saxena PK (eds) *Methods in Molecular Biology, Protocols for In Vitro Cultures and Secondary Metabolite Analysis of Aromatic and Medicinal Plants*. Humana Press, pp 337–345

Beretta GL, Petrangolini G, De Cesare M, Pratesi G, Perego P, Tinelli S, Tortoreto M, Zucchetti M, Frapolli R, Bello E, et al. (2006) Biological properties of IDN5174, a new synthetic camptothecin with the open lactone ring. *Cancer Res* 66: 10976–10982

Bodley AL, Cumming JN, Shapiro TA (1998) Effects of camptothecin, a topoisomerase I inhibitor, on *Plasmodium falciparum*. *Biochem Pharmacol* 55: 709–711

Bunsupa S, Okada T, Saito K, Yamazaki M (2011) An acyltransferase-like gene obtained by differential gene expression profiles of quinolizidine alkaloid-producing and nonproducing cultivars of *Lupinus angustifolius*. *Plant Biotechnol* 28: 89–94

Conesa A, Gotz S, Garcia-Gomez JM, Terol J, Talon M, Robles M (2005) Blast2GO: A universal tool for annotation, visualization and analysis in functional genomics research. *Bioinformatics* 21: 3674–3676

Fukushima A, Nakamura M, Suzuki H, Saito K, Yamazaki M (2015) High-throughput sequencing and *de novo* assembly of red and green forms of the *Perilla frutescens* var. *crispa* transcriptome. *PLoS ONE* 10: e0129154

Giovanella BC, Stehlin JS, Wall ME, Wani MC, Nicholas AW, Liu LF, Silber R, Potmesil M (1989) DNA topoisomerase I--targeted chemotherapy of human colon cancer in xenografts. *Science* 246: 1046–1048

Govindachari TR, Viswanathan N (1972) Alkaloids of *Mappia foetida*. *Phytochemistry* 11: 3529–3531

Grabherr MG, Haas BJ, Yassour M, Levin JZ, Thompson DA, Amit I, Adiconis X, Fan L, Raychowdhury R, Zeng Q, et al. (2011) Full-length transcriptome assembly from RNA-Seq data without a reference genome. *Nat Biotechnol* 29: 644–652

Han Y-S, Van der Heijden R, Verpoorte R (2001) Biosynthesis of anthraquinones in cell cultures of the Rubiaceae. *Plant Cell Tiss Org* 67: 201–220

Hsiang Y-H, Hertzberg R, Hecht S, Liu LF (1985) Camptothecin induced protein-linked DNA breaks via mammalian DNA topoisomerase I. *J Biol Chem* 260: 14873–14878

Hutchinson CR, Heckendorf AH, Straughn JL, Daddona PE, Cane DE (1979) Biosynthesis of camptothecin. 3. Definition of strictosamide as the penultimate biosynthetic precursor assisted by carbon-13 and deuterium NMR spectroscopy. *J Am Chem Soc* 101: 3358–3369

Kagale S, Links MG, Rozwadowski K (2010) Genome-wide analysis of ethylene-responsive element binding factor-associated amphiphilic repression motif-containing transcriptional regulators in Arabidopsis. *Plant Physiol* 152: 1109–1134

Kagale S, Rozwadowski K (2011) EAR motif-mediated transcriptional repression in plants. An underlying mechanism for epigenetic regulation of gene expression. *Epigenetics* 6: 141–146

Karwasara VS, Dixit VK (2012) Culture medium optimization for camptothecin production in cell suspension cultures of *Nothapodytes nimmoniana* (J. Grah.) Mabberley. *Plant Biotechnol Rep* 7: 357–369

Kitajima M, Fiscer U, Nakamura M, Ohsawa M, Ueno M, Takayama H, Unger M, Stockigt J, Aimi N (1998) Anthraquinones from *Ophiorrhiza pumila* tissue and cell cultures. *Phytochemistry* 48: 107–111

Kitajima M, Masumoto S, Takayama H, Aimi N (1997) Isolation and partial synthesis of 3(*R*)- and 3(*S*)-deoxypumiloside; structural revision of the key metabolite from the camptothecin producing plant, *Ophiorrhiza pumila*. *Tetrahedron Lett* 38: 4255–4258

Kranz HD, Denekamp M, Greco R, Jin H, Leyva A, Meissner RC,

Petroni K, Urzainqui A, Beva M, Martin C, et al. (1998) Towards functional characterisation of the members of the *R2R3-MYB* gene family from *Arabidopsis thaliana. Plant J* 16: 263–276

Kutchan TM (1995) Alkaloid biosynthesis - The basis for metabolic engineering of medicinal plants. *Plant Cell* 7: 1059–1070

Miettinen K, Dong L, Navrot N, Schneider T, Burlat V, Pollier J, Woittiez L, van der Krol S, Lugan R, Ilc T, et al. (2014) The seco-iridoid pathway from *Catharanthus roseus. Nat Commun* 5: 3606

Nakagawa T, Kurose T, Hino T, Tanaka K, Kawamukai M, Niwa Y, Toyooka K, Matsuoka K, Jinbo T, Kimura T (2007) Development of series of gateway binary vectors, pGWBs, for realizing efficient construction of fusion genes for plant transformation. *J Biosci Bioeng* 104: 34–41

Nakano Y, Yamaguchi M, Endo H, Rejab NA, Ohtani M (2015) NAC-MYB-based transcriptional regulation of secondary cell wall biosynthesis in land plants. *Front Plant Sci* 6: 288–306

Ni X, Wen S, Wang W, Wang X, Xu H, Kai G (2011) Enhancement of camptothecin production in *Camptotheca acuminata* hairy roots by overexpressing *ORCA3* gene. *J App Pharm Sci* 1: 85–88

Ohta M, Ohme-Takagi M, Shinshi H (2000) Three ethylene-responsive transcription factors in tobacco with distinct transactivation functions. *Plant J* 22: 29–38

Park YG, Kim MH, Yang JK, Chung YG, Choi MS (2003) Light-susceptibility of camptothecin production from *in vitro* cultures of *Camptotheca acuminata* Decne. *Biotechnol Bioproc E* 8: 32–36

Pauw B, Hilliou FA, Martin VS, Chatel G, de Wolf CJ, Champion A, Pré M, van Duijn B, Kijne JW, van der Fits L, Memelink J (2004) Zinc finger proteins act as transcriptional repressors of alkaloid biosynthesis genes in *Catharanthus roseus*. *J Biol Chem* 279: 52940–52948

Redinbo MR, Stewart L, Kuhn P, Champoux JJ, Hol WGJ (1998) Crystal structures of human topoisomerase I in covalent and noncovalent complexes with DNA. *Science* 279: 1504–1513

Saito K, Sudo H, Yamazaki M, Koseki-Nakamura M, Kitajima M, Takayama H, Aimi N (2001) Feasible production of camptothecin by hairy root culture of *Ophiorrhiza pumila. Plant Cell Rep* 20: 267–271

Sudo H, Yamakawa T, Yamazaki M, Aimi N, Saito K (2002) Bioreactor production of camptothecin by hairy root cultures of *Ophiorrhiza pumila*. *Biotechnol Lett* 24: 359–363

Tamagnone L, Merida A, Parr A, Mackay S, Culianez-Macia F, Roberts K, Martin C (1998) The AmMYB308 and AmMYB330 transcription factors from antirrhinum regulate phenylpropanoid and lignin biosynthesis in transgenic tobacco. *Plant Cell* 10: 135–154

Tamura K, Stecher G, Peterson D, Filipski A, Kumar S (2013) MEGA6: Molecular Evolutionary Genetics Analysis version 6.0. *Mol Biol Evol* 30: 2725–2729

Tanaka W, Toriba T, Ohmori Y, Yoshida A, Kawai A, Mayama-Tsuchida T, Ichikawa H, Mitsuda N, Ohme-Takagi M, Hirano HY (2012) The *YABBY* gene *TONGARI-BOUSHI1* is involved in lateral organ development and maintenance of meristem organization in the rice spikelet. *Plant Cell* 24: 80–95

Van der Fits L, Memelink J (2001) The jasmonate-inducible AP2/ERF-domain transcription factor ORCA3 activates gene expression via interaction with a jasmonate-responsive promoter element. *Plant J* 25: 43–53

Vincent RM, Lopez-Meyer M, McKnight TD, Nessler CL (1997) Sustained harvest of camptothecin from the leaves of *Camptotheca acuminata. J Nat Prod* 60: 618–619

Wall ME, Wani MC, Cook CE, Palmer KH, McPhail AT, Sim GA (1966) Plant anitumor agents I. The isolation and structure of camptothecin, a novel alkaloidal leukemia and tumor inhibitor from *Camptotheca acuminata. J Am Chem Soc* 88: 3888–3890

Werbovetz KA, Bhattacharjee AK, Brendle JJ, Scovill JP (2000) Analysis of stereoelectronic properties of camptothecin analogues in relation to biological activity. *Bioorg Med Chem* 8: 1741–1747

Wiseman LR, Markham A (1996) Irinoteca. A review of its pharmacological properties and clinical efficacy in the management of advanced colorectal cancer. *Drugs* 52: 606–623

Yamazaki M, Mochida K, Asano T, Nakabayashi R, Chiba M, Udomson N, Yamazaki Y, Goodenowe DB, Sankawa U, Yoshida T, et al. (2013) Coupling deep transcriptome analysis with untargeted metabolic profiling in *Ophiorrhiza pumila* to further the understanding of the biosynthesis of the anti-cancer alkaloid camptothecin and anthraquinones. *Plant Cell Physiol* 54: 686–696

Yamazaki Y, Sudo H, Yamazaki M, Aimi N, Saito K (2003) Camptothecin biosynthetic genes in hairy roots of *Ophiorrhiza pumila* cloning, characterization and differential expression in tissues and by stress compounds. *Plant Cell Physiol* 44: 395–403

Legends to supplementary figures

Supplementary Figure S1. *OpMYB1* expression in *OpMYB1*-overexpression in hairy roots (MYBox), compared to GUS lines. Each bar represents the mean ± SE of three biological replicates for each independent line.

Supplementary Figure S2. The camptothecin biosynthesis pathway and expression of contigs in *O. pumila*. The expression of contigs showed in red-yellow-green color scale and FPKM values. CSC, cell suspension culture; HR, hairy roots; MYBox, *OpMYB1*-overexpression in hairy roots; TDC, tryptophan decarboxylase; G10H, geraniol 10-hydroxylase; SLS, secologanin synthase; STR, strictosidine synthase. Dashed lines indicate unresolved reactions.

Supplementary Figure S3. The seco-iridoid biosynthesis pathway and expression of contigs in *O. pumila*. The expression levels of contigs showed in red-yellow-green color scale and FPKM values. CSC, cell suspension culture; HR, hairy roots; MYBox; *OpMYB1*-overexpression in hairy roots; IPP, isopentenyl pyrophosphate; DMAPP, dimethylallyl pyrophosphate; Glc, glucose; GPPS, geranyl diphosphate synthase; GES, geraniol synthase; G10H, geraniol 10-hydroxylase; 10-HGO, 10-hydroxygeraniol dehydrogenase; IS, iridoid synthase; IO, iridoid oxidase; 7-DLGT, 7-deoxyloganetic acid glucosyl transferase; 7-DLH, 7-deoxyloganic acid hydroxylase; LAMT, loganic acid *O*-methyltransferase; SLS, secologanin synthase; STR, strictosidine synthase; TDC, tryptophan decarboxylase.

Supplementary Figure S4. The anthraquinone biosynthesis pathway and expression of contigs in *O. pumila*. The expression levels of contigs showed in red-yellow-green color scale and FPKM values. CSC, cell suspension culture; HR, hairy roots; MYBox; *OpMYB1*-overexpression in hairy roots; MenF; menaquinone-specific isochorismate synthase; MenD, 2-succinyl-5-enolpyruvyl-6-hydroxy-3-cyclohexene-1-carboxylate synthase; MenH, 2-succinyl-6-hydroxy-2,4-cyclohexadiene-1-carboxylate synthase; MenC, *o*-succinyl benzoate synthase; MenE, *o*-succinyl benzoic acid-CoA ligase; MenB, naphthoate synthase; DXPS, 1-deoxy-D-xylulose-5-phosphate synthase; CLA, cloroplastos alterados; DXR, 1-deoxy-D-xylulose 5-phosphate reductoisomerase; ISPD, 2-*C*-methyl-D-erythritol 4-phosphate cytidylyltransferase; CDPMEK, 4-diphosphocytidyl-2-*C*-methyl-D-erythritol kinase; ISPF, 2-*C*-methyl-D-erythritol 2,4-cyclodiphosphate synthase; HDS, (*E*)-4-hydroxy-3-methylbut-2-enyl diphosphate synthase; HDR, 4-hydroxy-3-methylbut-2-enyl diphosphate reductase.

Supplementary Figure S5. The chlorogenic acid biosynthesis pathway and expression of contigs in *O. pumila*. The expression levels of contigs showed in red-yellow-green color scale and FPKM values. CSC, cell suspension culture; HR, hairy roots; MYBox, *OpMYB1*-overexpression in hairy roots; HQT, hydroxycinnamoyl-CoA quinate hydroxycinnamoyl transferase; CYP98A35 or C3H1, *p*-coumaroyl quinate/shikimate 3′-hydroxylase; Quinate HCT, caffeoyl-CoA:quinate *O*-(hydroxycinnamoyl) transferase; CCoAOMT1, caffeoyl-CoA 3-*O*-methyl transferase.

Supplementary Figure S1

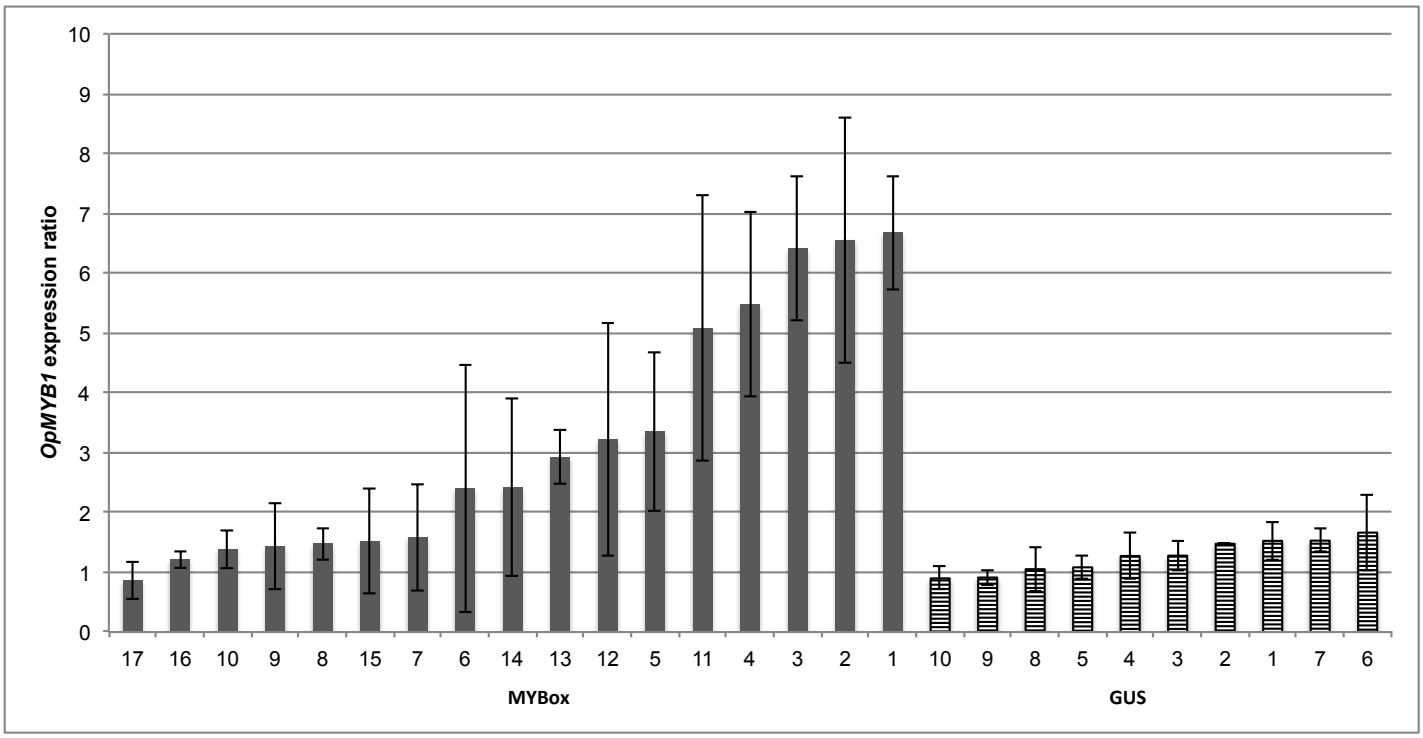

Supplementary Figure S2

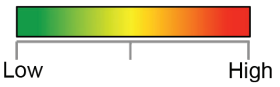

G10H	CSC	HR	MYBox
c28312_g1_i1	7.78	303.73	176.74

SLS	CSC	HR	MYBox
c20052_g2_i1	0.00	4.40	1.04
c32866_g1_i1	19.93	38.82	53.31
c19494_g1_i1	0.00	3.55	2.47
c31777_g2_i1	14.35	50.05	24.64
c31777_g2_i2	0.00	20.71	10.68
c31777_g2_i3	5.92	2.53	15.27
c31777_g3_i1	9.00	45.30	19.49
c31777_g4_i1	17.84	68.66	39.97
c21692_g2_i1	0.32	61.88	53.40
c32840_g2_i1	104.28	155.81	111.61
c8923_g1_i1	0.00	60.25	58.97
c32845_g1_i1	5.93	10.14	14.52
c32845_g2_i2	0.00	3.48	3.05
c30629_g2_i4	3.70	3.39	4.76
c41889_g1_i1	0.34	633.51	467.91
c27549_g1_i1	0.00	59.07	39.00
c27549_g2_i1	0.00	39.61	23.33
c46469_g1_i1	0.00	0.74	7.03
c4041_g1_i1	0.00	1.22	3.77
c7287_g1_i1	1.34	81.21	47.53

STR	CSC	HR	MYBox
c47430_g1_i1	0.12	962.27	707.96
c20528_g2_i1	0.00	13.25	18.06
c11848_g1_i1	0.00	0.00	12.48
c980_g1_i1	2.68	0.88	4.61
c32972_g2_i1	0.81	1.87	4.43
c32972_g1_i1	0.00	39.29	11.14
c20528_g1_i1	0.00	2.54	0.00
c20528_g3_i1	0.00	5.62	5.12
c18195_g1_i1	0.00	19.87	9.31
c18195_g1_i2	0.00	3.62	3.61
c34331_g1_i1	0.00	144.43	31.38
c32972_g3_i1	0.00	0.69	9.25
c34166_g1_i1	0.00	11.07	4.98
c8855_g1_i1	0.00	2.15	4.05
c22607_g1_i1	11.22	3.42	4.00
c45990_g1_i1	0.00	3.29	1.51
c24194_g1_i1	0.00	196.23	68.72
c10375_g1_i1	0.00	0.24	14.63
c37461_g1_i1	0.00	1.31	6.06
c32972_g4_i1	0.00	1.76	5.44
c25181_g1_i1	0.00	12.04	13.26
c44002_g1_i1	0.00	3.03	0.96
c26065_g1_i1	0.00	10.03	0.85

TDC	CSC	HR	MYBox
c18285_g2_i1	0.00	0.00	4.95
c28648_g1_i1	0.12	537.14	324.28
c28893_g1_i1	0.00	11.71	2.86
c3779_g1_i1	0.00	15.30	6.32
c39640_g1_i1	0.00	2.96	1.44
c43018_g1_i1	0.00	7.69	0.51
c44343_g1_i1	0.00	1.29	2.40

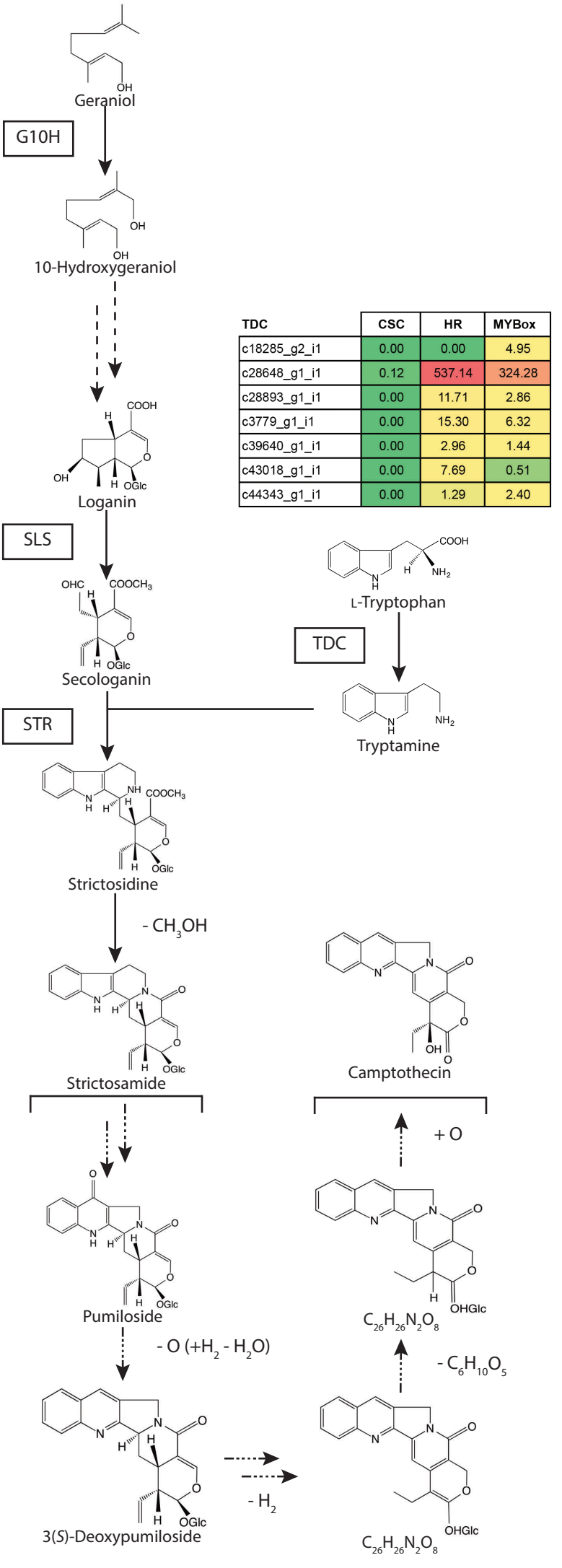

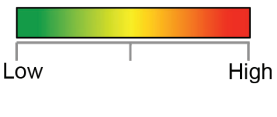

GPPS	CSC	HR	MYBox
c32449_g1_i1	1.01	8.70	4.60
c32449_g1_i2	0.26	25.21	14.95
c32644_g1_i2	5.85	1.26	1.31
c32644_g1_i3	16.69	24.79	23.36
c48032_g1_i1	0.00	2.67	1.94
c33163_g3_i1	26.01	13.62	16.38
c25825_g1_i1	5.47	25.53	22.17
c17006_g1_i1	6.51	21.40	9.73

GES	CSC	HR	MYBox
c36701_g1_i1	6.64	39.68	29.39

G10H	CSC	HR	MYBox
c28312_g1_i1	7.78	303.73	176.74

10-HGO	CSC	HR	MYBox
c31297_g1_i1	0.00	125.77	73.57
c29140_g1_i1	32.83	223.05	139.37

IS	CSC	HR	MYBox
c42337_g1_i1	18.78	281.15	147.10

IO	CSC	HR	MYBox
c39235_g1_i1	108.79	372.33	284.42

7-DLGT	CSC	HR	MYBox
c22992_g1_i1	8.73	3.97	5.82
c22992_g2_i1	18.72	18.54	19.54
c22992_g3_i1	37.37	27.39	33.17
c25318_g2_i1	0.00	1.78	3.65
c25318_g2_i2	0.26	0.74	1.58
c38432_g1_i1	15.63	58.95	42.22
c18121_g1_i1	7.19	41.38	20.48
c1241_g1_i1	0.00	0.70	3.73
c30764_g1_i1	7.54	13.29	12.55
c24002_g1_i1	6.38	70.43	36.57
c18473_g1_i1	3.59	50.77	52.84

7-DLH	CSC	HR	MYBox
c18879_g1_i1	11.86	176.98	113.63
c18879_g2_i1	8.90	85.91	42.65
c18879_g3_i1	8.66	110.45	57.57
c4068_g1_i1	0.00	25.89	9.31
c4068_g1_i2	0.00	139.31	1.78

LAMT	CSC	HR	MYBox
c5842_g1_i1	0.00	175.82	104.10

SLS	CSC	HR	MYBox
c20052_g2_i1	0.00	4.40	1.04
c32866_g1_i1	19.93	38.82	53.31
c19494_g1_i1	0.00	3.55	2.47
c31777_g2_i1	14.35	50.05	24.64
c31777_g2_i2	0.00	20.71	10.68
c31777_g2_i3	5.92	2.53	15.27
c31777_g3_i1	9.00	45.30	19.49
c31777_g4_i1	17.84	68.66	39.97
c21692_g2_i1	0.32	61.88	53.40
c32840_g2_i1	104.28	155.81	111.61
c8923_g1_i1	0.00	60.25	58.97
c32845_g1_i1	5.93	10.14	14.52
c32845_g2_i2	0.00	3.48	3.05
c30629_g2_i4	3.70	3.39	4.76
c41889_g1_i1	0.34	633.51	467.91
c27549_g1_i1	0.00	59.07	39.00
c27549_g2_i1	0.00	39.61	23.33
c46469_g1_i1	0.00	0.74	7.03
c4041_g1_i1	0.00	1.22	3.77
c7287_g1_i1	1.34	81.21	47.53

TDC	CSC	HR	MYBox
c18285_g2_i1	0.00	0.00	4.95
c28648_g1_i1	0.12	537.14	324.28
c28893_g1_i1	0.00	11.71	2.86
c3779_g1_i1	0.00	15.30	6.32
c39640_g1_i1	0.00	2.96	1.44
c43018_g1_i1	0.00	7.69	0.51
c44343_g1_i1	0.00	1.29	2.40

STR	CSC	HR	MYBox
c47430_g1_i1	0.12	962.27	707.96
c20528_g2_i1	0.00	13.25	18.06
c11848_g1_i1	0.00	0.00	12.48
c980_g1_i1	2.68	0.88	4.61
c32972_g2_i1	0.81	1.87	4.43
c32972_g1_i1	0.00	39.29	11.14
c20528_g1_i1	0.00	2.54	0.00
c20528_g3_i1	0.00	5.62	5.12
c18195_g1_i1	0.00	19.87	9.31
c18195_g1_i2	0.00	3.62	3.61
c34331_g1_i1	0.00	144.43	31.38
c32972_g3_i1	0.00	0.69	9.25
c34166_g1_i1	0.00	11.07	4.98
c8855_g1_i1	0.00	2.15	4.05
c22607_g1_i1	11.22	3.42	4.00
c45990_g1_i1	0.00	3.29	1.51
c24194_g1_i1	0.00	196.23	68.72
c10375_g1_i1	0.00	0.24	14.63
c37461_g1_i1	0.00	1.31	6.06
c32972_g4_i1	0.00	1.76	5.44
c25181_g1_i1	0.00	12.04	13.26
c44002_g1_i1	0.00	3.03	0.96
c26065_g1_i1	0.00	10.03	0.85

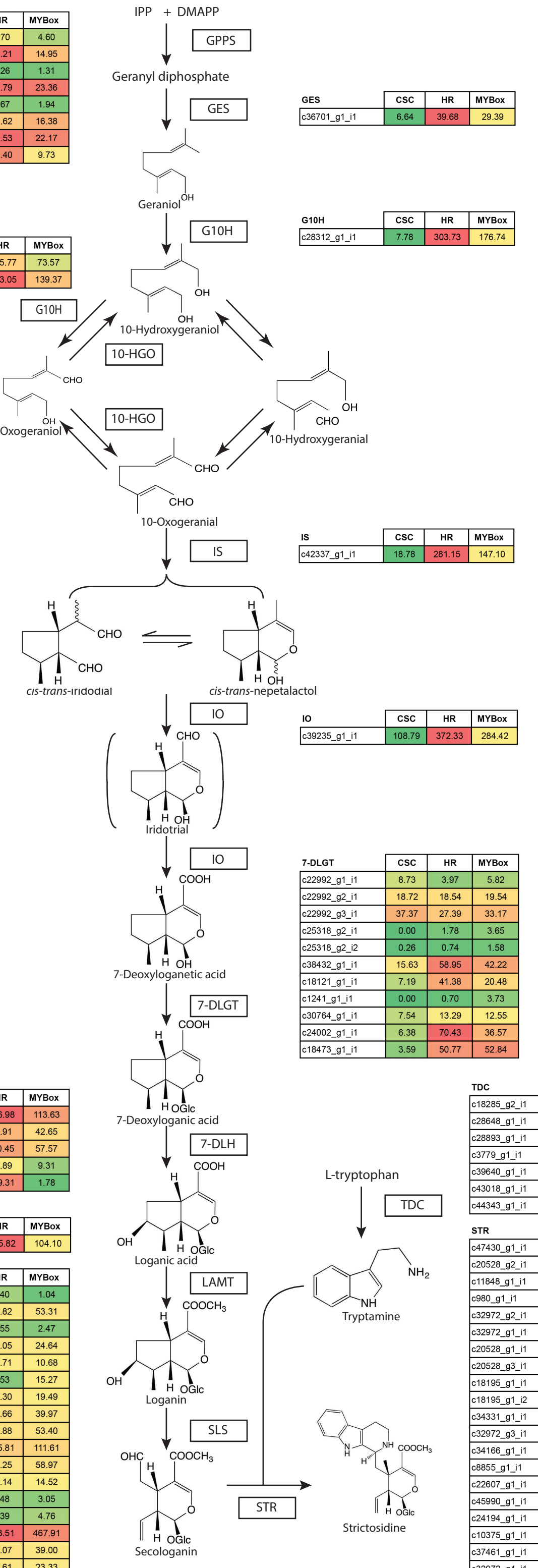

Supplementary Figure S4

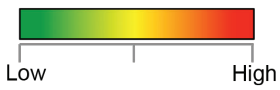

MenF	CSC	HR	MYBox
c33856_g1_i1	1.47	161.95	124.39

MenD	CSC	HR	MYBox
c33442_g6_i1	1.99	79.32	46.73

MenC	CSC	HR	MYBox
c22217_g1_i1	1.75	398.92	291.76

MenE	CSC	HR	MYBox
c32537_g1_i1	0.00	0.00	1.75
c810_g1_i1	0.00	2.55	4.56
c47809_g1_i1	0.34	0.37	5.47
c25763_g1_i1	8.18	17.03	12.38
c31684_g1_i1	4.97	22.63	19.87
c32537_g1_i3	9.57	17.97	21.08
c22993_g1_i1	88.78	76.76	72.00
c22627_g1_i1	1028.13	182.70	156.65

MenB	CSC	HR	MYBox
c33824_g1_i1	5.17	596.95	420.25

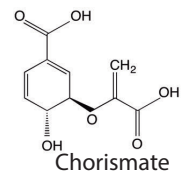
Chorismate

MenF

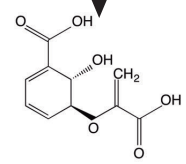
Isochorismate

MenD

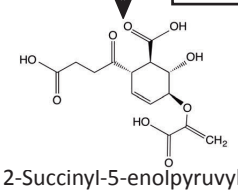
2-Succinyl-5-enolpyruvyl-6-hydroxy-3-cyclohexene-1-carbo=xylate

MenH

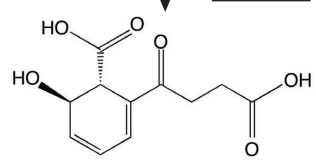
(1R,6R)-2-Succinyl-6-hydroxy-2,4-cyclohexadiene-1-carboxylate

MenC

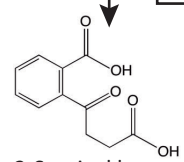
2-Succinyl benzoate

MenE

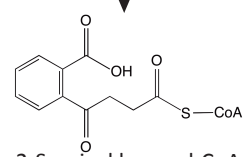
2-Succinyl benzoyl-CoA

MenB

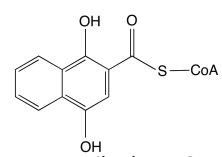
1,4-Dihydroxy-2-naphthoyl-CoA

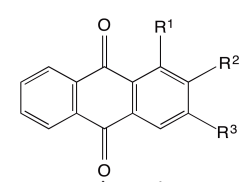
Anthraquinone

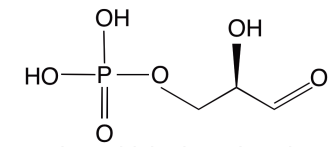
D-Glyceraldehyde 3-phosphate

DXPS1,DXPS3, CLA1

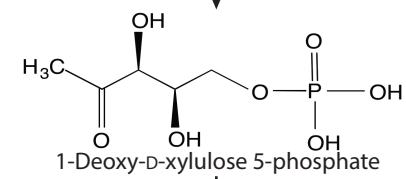
1-Deoxy-D-xylulose 5-phosphate

DXR

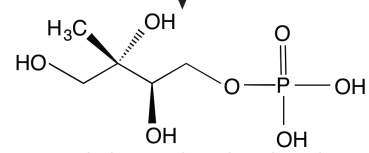
2-C-Methyl-D-erythritol 4-phosphate

ISPD

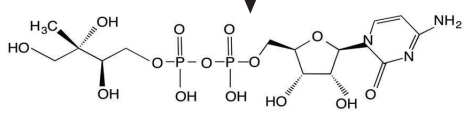
4-(Cytidine 5’-diphospho)-2-C-methyl-D-erythritol

CDPMEK

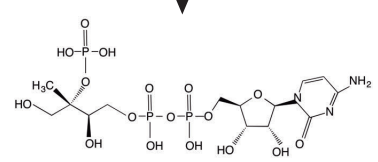
2-Phospho-4-(cytidine 5’-diphospho)-2-C-methyl-D-erythritol

ISPF

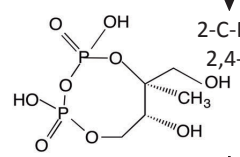
2-C-Methyl-D-erythritol 2,4-cyclodiphosphate

HDS

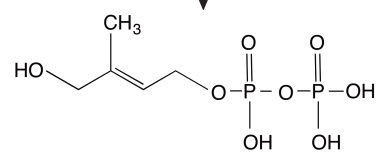
1-Hydroxy-2-methyl-2-butenyl 4-diphosphate

HDR

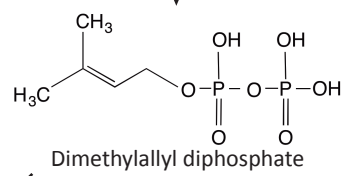
Dimethylallyl diphosphate

DXPS3, CLA1	CSC	HR	MYBox
c29996_g1_i1	7.96	164.02	148.77
c29282_g2_i1	0.11	53.36	36.04
c29282_g1_i1	0.00	47.14	39.31
c29855_g1_i2	8.70	10.17	8.88
c29855_g1_i1	0.81	1.80	3.72
c38641_g1_i1	1.44	1.76	1.59
c30018_g3_i2	0.78	1.29	1.89
c30018_g1_i1	8.16	6.30	11.04
c30018_g3_i3	7.95	4.37	5.89

DXR	CSC	HR	MYBox
c33486_g7_i1	123.83	179.17	144.07
c33486_g1_i5	21.53	13.81	9.57
c33486_g1_i3	0.85	2.74	2.06

ISPD	CSC	HR	MYBox
c23841_g1_i1	25.29	26.30	17.55

CDPMEK	CSC	HR	MYBox
c28782_g1_i1	13.36	50.01	33.87

ISPF	CSC	HR	MYBox
c17510_g1_i1	103.23	174.71	155.63

HDS	CSC	HR	MYBox
c23444_g2_i1	80.68	255.50	217.53

HDR	CSC	HR	MYBox
c17511_g1_i1	82.98	278.72	185.97
c5100_g1_i1	6.04	5.40	5.19

Supplementary Figure S5

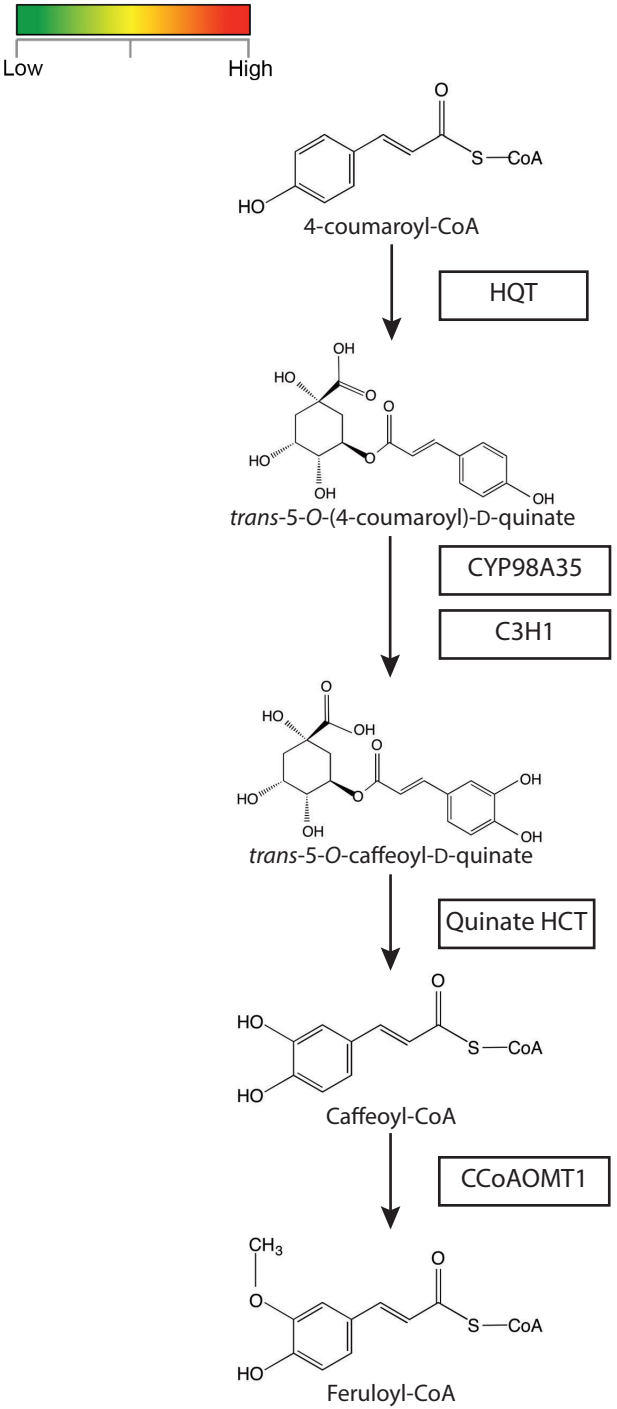

HQT	CSC	HR	MYBox
c17064_g1_i1	12.03	93.74	33.36

CYP98A35 / C3H1	CSC	HR	MYBox
c24241_g1_i1	2.74	83.93	29.39
c24241_g2_i1	4.95	116.26	53.83
c26370_g1_i1	36.70	235.14	117.51

Quinate HCT	CSC	HR	MYBox
c23775_g2_i1	0.00	7.49	0.16
c23775_g1_i1	0.00	10.28	0.72
c22655_g1_i1	0.00	0.81	1.55
c15374_g1_i2	0.21	8.30	5.36
c7976_g1_i1	1.25	12.99	8.00
c15374_g1_i1	0.00	28.00	19.80
c30394_g3_i1	0.00	56.42	21.27
c23181_g1_i1	0.00	259.05	110.00

CCoAOMT1	CSC	HR	MYBox
c20243_g1_i2	0.21	0.91	2.27
c25259_g1_i3	0.78	2.83	5.42
c25259_g1_i1	1.26	5.27	6.79
c39211_g1_i1	6.55	209.71	175.68
c41891_g1_i1	100.27	516.95	156.67
c32955_g1_i2	2.86	1.26	1.38

Supplementary Tables

Supplementary Table S1. List of primers used for vector construction in this study.

Primer Name	Sequence
OpMYB1-ORF-attB1-F	AAA AAG CAG GCT CTA TGG GAC GTT CAC CTT GCT GTG
OpMYB1-ORF-attB2-R	AGA AAG CTG GGT TGT ATC TGT ATA CAC CAT TTG CCA TTT C

Supplementary Table S2. List of primers used for semi-quantitative RT-PCR

Target Gene	Primer Name	Sequence
OpMYB1	OpMYB1-F	CAA CAA CGA TCA AAA CAG CA
	OpMYB1-R	GGA TTC AGC TGA AGT AGT AGT
OpTDC	OpTDC-F	ATG GGC AGC ATT AGT GAA AA
	OpTDC-R	TTA CTC AAT GAT ATT GGT TTT CGT
OpG10H	OpG10H-F	AGA TTT AGC TTT CTC CAG CCG
	OpG10H-R	TAT CAA TAA GGG GCC AAC CA
OpSTR	OpSTR-F	ATG CAT AGT TCA GAA GCC AT
	OpSTR-R	TCA GAA AGA AGA AAA TTC CTT G
OpSLS	OpSLS-F	TCA TGC CTC ATA TTG ACC ACA
	OpSLS-R	GGA TGG TGA AAC ATC AAA GGT
OpTub	OpTub-F	CCA GAT AAC TTT GTT TTC GG
	OpTub-R	GTG AAC TCC ATT TCA TCC AT

Supplementary Table S3. Gene fragments of transcription factor isolated from *O. pumila* hairy root.

Annotation (BLASTx analysis)	No. of gene fragments
MYB	1
Putative bHLH transcription factor	1
Root-specific gene regulator	2
Putative BURP domain containing protein	2
Putative zinc finger protein	3
ERF-like protein	6

Supplementary Table S4. Accession numbers of genes used for phylogenetic tree analysis

Protein Name	Plant Species	Accession number
AtMYB4	*Arabidopsis thaliana*	NP_195574.1
BrMYB4	*Brassica rapa*	XP_009101934.1
AtMYB3	*Arabidopsis thaliana*	NP_564176
PdMYB308	*Phoenix dactylifera*	XP_008783376.1
AmMYB308	*Antirrhinum majus*	P81393
AcMYB1	*Actinidia chinensis*	AHB17741.1
GaMYB	*Gossypium arboretum*	KHG25834.1
MnMYB	*Morus notabilis*	XP_010104477.1
CmMYB6	*Cucumis melo*	XP_008459665.1
CsMYB6	*Cucumis sativus*	XP_004141649.1
CmMYB1	*Cucumis melo*	XP_008459665.1
GhMYB8	*Gossypium hirsutum*	ABR01221.1
GaMYB3	*Gossypium arboretum*	KHG11058.1
FvMYB6	*Fragaria vesca*	XP_004299892.1
CsMYB330	*Citrus sinensis*	XP_006473170.1
EsMYB1	*Epimedium sagittatum*	AFH03053.1
OpMYB1	*Ophiorrhiza pumila*	LC076107
SiMYB330	*Sesamum indicum*	XP_011096483.1
PmMYB6	*Prunus mume*	XP_008219033.1
MdMYB3	*Malus domestica*	AEX08668.1
SmMYB	*Salvia miltiorrhiza*	AGN52078.1
AmMYB330	*Antirrhinum majus*	P81395.1
GhMYB1	*Gossypium hirsutum*	AAA33067.1
GrMYB6	*Gossypium raimondii*	XP_012462415.1
NnMYB330	*Nelumbo nucifera*	XP_010246045.1
GsMYB308	*Glycine soja*	KHN09677.1
JcMYB6	*Jatropha curcas*	XP_012075785.1
RcMYB	*Riccinus communis*	XP_002534486.1
PeMYB6	*Populus euphratica*	XP_011001099.1
PtMYB	*Populus trichocarpa*	XP_002325546.1
TcMYB	*Theobroma cacao*	XP_007020033.1
SlMYB330	*Solanum lycopersicum*	XP_004241841.1
LeMYB2	*Lithospermum erythrorhizon*	AIS39993.1
EgMYB330	*Erythranthe guttatus*	XP_012854909.1
NsMYB330	*Nicotiana sylvestris*	XP_009767902.1
NtMYB330	*Nicotiana tomentosiformis*	XP_009600359.1
StMYB330	*Solanum tuberosum*	XP_006356500.1
AtMYBL2	*Arabidopsis thaliana*	NP_177259
GrMYB1	*Gossypium raimondii*	AAN28271.1
MtMYB2	*Medicago truncatula*	ABR28329

Supplementary Table S5. Differential GO enrichment for MYBox in *O. pumila* .

GO-ID	Term	FDR	*P* -Value	No. of differentially expressed genes
GO:0003824	catalytic activity	3.86E-09	1.22E-11	2762
GO:0046906	tetrapyrrole binding	5.42E-08	2.01E-10	176
GO:0020037	heme binding	1.10E-07	4.21E-10	170
GO:0016491	oxidoreductase activity	1.32E-07	5.25E-10	641
GO:0016705	oxidoreductase activity, acting on paired donors, with incorporation or reduction of molecular oxygen	1.99E-07	8.19E-10	207
GO:0004497	monooxygenase activity	5.88E-07	2.74E-09	130
GO:0019748	secondary metabolic process	2.06E-06	1.05E-08	84
GO:0055114	oxidation-reduction process	8.93E-06	5.27E-08	592
GO:0009698	phenylpropanoid metabolic process	1.24E-04	1.11E-06	45
GO:0016709	oxidoreductase activity, acting on paired donors, with incorporation or reduction of molecular oxygen, N	2.07E-04	2.02E-06	51
GO:0005215	transporter activity	2.82E-04	2.90E-06	373
GO:0022804	active transmembrane transporter activity	3.85E-04	4.02E-06	171
GO:0044550	secondary metabolite biosynthetic process	7.27E-04	7.78E-06	52
GO:0004601	peroxidase activity	1.18E-03	1.39E-05	48
GO:0016684	oxidoreductase activity, acting on peroxide as acceptor	1.18E-03	1.39E-05	48
GO:0022857	transmembrane transporter activity	1.69E-03	2.20E-05	293
GO:0006979	response to oxidative stress	2.29E-03	3.05E-05	107
GO:0019187	beta-1,4-mannosyltransferase activity	3.19E-03	4.51E-05	11
GO:0005506	iron ion binding	4.63E-03	6.92E-05	151
GO:0006820	anion transport	4.63E-03	6.98E-05	114
GO:0016682	oxidoreductase activity, acting on diphenols and related substances as donors, oxygen as acceptor	4.86E-03	7.46E-05	24
GO:0008762	UDP-N-acetylmuramate dehydrogenase activity	4.87E-03	7.55E-05	34
GO:0005576	extracellular region	5.70E-03	9.07E-05	151
GO:0055085	transmembrane transport	9.16E-03	1.53E-04	345
GO:0051213	dioxygenase activity	9.48E-03	1.60E-04	70
GO:0009521	photosystem	9.68E-03	1.66E-04	43
GO:0015276	ligand-gated ion channel activity	1.01E-02	1.77E-04	20
GO:0022834	ligand-gated channel activity	1.01E-02	1.77E-04	20
GO:0051753	mannan synthase activity	1.24E-02	2.17E-04	9
GO:0016840	carbon-nitrogen lyase activity	1.29E-02	2.28E-04	19
GO:0016209	antioxidant activity	1.43E-02	2.57E-04	51
GO:0042626	ATPase activity, coupled to transmembrane movement of substances	1.51E-02	2.73E-04	93
GO:0009522	photosystem I	1.70E-02	3.20E-04	30
GO:0043492	ATPase activity, coupled to movement of substances	1.70E-02	3.18E-04	94
GO:0016787	hydrolase activity	1.72E-02	3.31E-04	968
GO:0046271	phenylpropanoid catabolic process	1.72E-02	3.37E-04	15
GO:0046274	lignin catabolic process	1.72E-02	3.37E-04	15
GO:0052716	hydroquinone:oxygen oxidoreductase activity	1.72E-02	3.37E-04	15
GO:0010295	(+)-abscisic acid 8'-hydroxylase activity	1.91E-02	3.78E-04	5
GO:0050660	flavin adenine dinucleotide binding	2.14E-02	4.37E-04	71
GO:0048767	root hair elongation	2.26E-02	4.67E-04	29
GO:0016820	hydrolase activity, acting on acid anhydrides, catalyzing transmembrane movement of substances	2.56E-02	5.34E-04	93
GO:0015297	antiporter activity	2.63E-02	5.53E-04	54
GO:0016144	S-glycoside biosynthetic process	2.82E-02	6.12E-04	26
GO:0019758	glycosinolate biosynthetic process	2.82E-02	6.12E-04	26
GO:0019761	glucosinolate biosynthetic process	2.82E-02	6.12E-04	26
GO:0016843	amine-lyase activity	3.63E-02	8.17E-04	12
GO:0016844	strictosidine synthase activity	3.63E-02	8.17E-04	12
GO:0016887	ATPase activity	3.63E-02	8.21E-04	198
GO:0006857	oligopeptide transport	3.75E-02	8.63E-04	28
GO:0006811	ion transport	4.01E-02	9.56E-04	251
GO:0009808	lignin metabolic process	4.25E-02	1.03E-03	25
GO:0015291	secondary active transmembrane transporter activity	4.25E-02	1.03E-03	78
GO:0016679	oxidoreductase activity, acting on diphenols and related substances as donors	4.25E-02	1.03E-03	25
GO:0044765	single-organism transport	4.57E-02	1.12E-03	489
GO:0004499	N,N-dimethylaniline monooxygenase activity	4.63E-02	1.15E-03	17
GO:1902578	single-organism localization	4.92E-02	1.24E-03	497

Supplementary Table S6. Supporting information from BLAST search of contigs in Figure 7.

Biosynthesis	Enzyme	Contig ID	FPKM			Contig Length	#Hits	E-Value	Mean Similarity (%)	#GOs	GOs	Enzyme Codes
			CSC	HR	MYBox							
Camptothecin	TDC	c18285_g2_i1	0	0	4.95	217	10	1.98E-39	93.40%	3	F:pyridoxal ph	EC:4.1.1.28
		c28648_g1_i1	0.116	537.142	324.278	1933	10	0	86.40%	3	F:pyridoxal ph	EC:4.1.1.28
		c28893_g1_i1	0	11.711	2.864	1409	10	0	86.30%	3	F:pyridoxal ph	EC:4.1.1.28
		c3779_g1_i1	0	15.303	6.317	443	10	4.65E-70	80.40%	3	F:pyridoxal ph	EC:4.1.1.28
		c39640_g1_i1	0	2.959	1.437	429	10	2.32E-71	86.10%	3	F:pyridoxal ph	EC:4.1.1.28
		c43018_g1_i1	0	7.693	0.509	639	10	7.15E-54	82.50%	3	F:pyridoxal ph	EC:4.1.1.28
		c44343_g1_i1	0	1.287	2.395	288	10	3.25E-26	83.80%	3	F:pyridoxal ph	EC:4.1.1.28
	G10H	c28312_g1_i1	7.779	303.734	176.74	1770	10	0	86.30%	8	C:endoplasmic	EC:1.14.14.1; EC:1.14.13
	SLS	c32866_g1_i1	19.93	38.818	53.314	1445	10	0	82.00%	6	F:heme bindin	EC:1.3.3.9
		c31777_g2_i1	14.351	50.051	24.641	331	10	5.66E-43	82.40%	5	F:heme bindin	-
		c31777_g2_i2	0	20.712	10.679	331	10	1.99E-43	82.40%	5	F:heme bindin	-
		c31777_g3_i1	8.995	45.296	19.491	367	10	6.46E-63	83.20%	8	F:secologanin	EC:1.3.3.9
		c31777_g4_i1	17.835	68.656	39.971	245	10	5.27E-38	86.90%	5	F:heme bindin	-
		c21692_g2_i1	0.318	61.876	53.404	524	10	2.07E-85	80.30%	5	F:heme bindin	-
		c32840_g2_i1	104.281	155.812	111.609	1838	10	0	80.50%	5	F:heme bindin	-
		c8923_g1_i1	0	60.246	58.973	223	10	6.79E-28	81.90%	5	F:heme bindin	-
		c41889_g1_i1	0.338	633.507	467.914	2061	10	0	91.60%	9	F:secologanin	EC:1.3.3.9
		c27549_g1_i1	0	59.073	39.003	275	10	1.16E-16	81.80%	9	F:secologanin	EC:1.3.3.9
		c27549_g2_i1	0	39.607	23.334	1477	10	0	89.00%	9	F:secologanin	EC:1.3.3.9
		c7287_g1_i1	1.342	81.208	47.526	270	10	7.17E-11	89.80%	5	F:heme bindin	-
	STR	c47430_g1_i1	0.116	962.272	707.959	1120	10	0	83.10%	2	P:biosynthetic p	EC:4.3.3.2
		c20528_g2_i1	0	13.247	18.064	362	10	4.55E-22	61.90%	2	P:biosynthetic process; F:strictosidine synthase activity	
		c32972_g1_i1	0	39.285	11.138	1070	10	4.27E-86	56.30%	1	C:cell part	-
		c18195_g1_i1	0	19.871	9.312	1359	10	8.64E-100	65.10%	4	C:cytoplasmic p	-
		c34331_g1_i1	0	144.434	31.378	1341	10	4.47E-71	55.30%	1	C:cell part	-
		c24194_g1_i1	0	196.229	68.724	1269	10	1.22E-107	60.60%	3	C:cell part; F:str	-
		c26065_g1_i1	0	10.029	0.848	593	10	1.78E-50	76.80%	2	F:strictosidine sy	EC:4.3.3.2
Seco-iridoid	GPPS	c32449_g1_i1	1.013	8.7	4.601	1480	10	1.11E-179	75.30%	9	F:metal ion bir	EC:2.5.1.1; EC:2.5.1.29; EC:2.5.1.10
		c32449_g1_i2	0.261	25.207	14.95	1658	10	0	80.60%	9	F:metal ion bind	EC:2.5.1.1; EC:2.5.1.29; EC:2.5.1.10
		c32644_g1_i3	16.687	24.792	23.364	1782	10	0	84.50%	5	P:embryo devel	EC:2.5.1.1; EC:2.5.1.30
		c48032_g1_i1	0	2.668	1.936	1294	10	5.99E-152	82.50%	10	F:metal ion bind	EC:2.5.1.1; EC:2.5.1.29; EC:2.5.1.30; EC:2.5.1.10
		c33163_g3_i1	26.01	13.621	16.378	1652	10	0	76.50%	6	P:response to s	EC:2.5.1.29
		c25825_g1_i1	5.472	25.529	22.166	1534	10	0	78.20%	7	F:geranyltranst	EC:2.5.1.1; EC:2.5.1.29; EC:2.5.1.30; EC:2.5.1.10
		c17006_g1_i1	6.505	21.397	9.731	563	10	4.12E-51	67.60%	4	P:terpenoid bi	EC:2.5.1
		c32644_g1_i2	5.849	1.256	1.307	1850	10	1.67E-156	79.20%	2	P:isoprenoid b	EC:2.5.1.1
	GES	c36701_g1_i1	6.64	39.68	29.392	1868	10	0	80.80%	7	F:terpene synth	EC:3.1.7.3
	G8O	c28312_g1_i1	7.779	303.734	176.74	1770	10	0	86.30%	8	C:endoplasmic	EC:1.14.14.1; EC:1.14.13
	8-HGO	c31297_g1_i1	0	125.767	73.574	1687	10	1.26E-142	70.70%	4	F:oxidoreducta	-
		c29140_g1_i1	32.833	223.046	139.374	1825	10	0	79.70%	4	F:zinc ion bind	EC:1.1.1.1
	IS	c42337_g1_i1	18.781	281.154	147.099	1600	10	0	66.50%	4	P:monoterpen	-
	IO	c39235_g1_i1	108.788	372.328	284.417	1928	10	0	72.70%	5	F:oxidoreducta	-
	7-DLGT	c22992_g1_i1	8.725	3.966	5.818	541	10	5.08E-36	87.60%	2	F:transferase a	-
		c22992_g2_i1	18.723	18.542	19.541	831	10	2.11E-113	80.50%	2	F:transferase a	-
		c22992_g3_i1	37.369	27.388	33.174	529	10	3.27E-101	88.90%	2	F:transferase a	-
		c25318_g2_i1	0	1.775	3.653	606	10	9.54E-57	82.90%	2	F:transferase a	-

		c25318_g2_i2	0.261	0.737	1.577	593	10	4.46E-97	84.50%	2	F:transferase a
		c38432_g1_i1	15.625	58.949	42.216	521	10	8.19E-90	84.10%	2	F:transferase a
		c18121_g1_i1	7.19	41.382	20.479	1360	10	0	92.00%	2	F:transferase a
		c1241_g1_i1	0	0.696	3.733	525	10	8.27E-25	69.50%	2	F:transferase a
		c30764_g1_i1	7.538	13.289	12.545	1891	10	0	77.50%	2	F:transferase a
		c24002_g1_i1	6.379	70.431	36.568	1212	10	5.70E-141	70.30%	2	P:metabolic pr
		c18473_g1_i1	3.59	50.768	52.835	1887	10	0	76.30%	2	F:transferase a
	7-DLH	c18879_g1_i1	11.861	176.981	113.625	661	10	1.91E-134	85.60%	4	F:heme bindin
		c18879_g2_i1	8.898	85.911	42.646	699	10	4.20E-61	92.20%	5	F:heme bindin
		c18879_g3_i1	8.657	110.454	57.566	689	10	3.34E-120	83.10%	5	F:iron ion bind
		c4068_g1_i1	0	25.893	9.312	1953	10	0	78.40%	4	F:heme bindin
		c4068_g1_i2	0	139.305	1.776	1954	10	0	78.40%	4	F:heme bindin
	LAMT	c5842_g1_i1	0	175.818	104.104	1469	10	0	68.40%	2	P:methylation;
Anthraquinone	MenF	c33856_g1_i1	1.467	161.948	124.394	2342	10	0	76.30%	3	F:isochorismat
		c32294_g2_i1	17.324	55.938	29.512	1868	10	0	81.30%	5	C:nucleolus; P
		c32294_g2_i2	53.911	44.892	48.714	2162	10	0	86.60%	5	C:nucleolus; P
	MenD	c33442_g6_i1	1.988	79.318	46.727	4360	10	0	72.80%	7	F:hydrolase ac
	MenC	c22217_g1_i1	1.747	398.916	291.762	2293	10	0	71.00%	1	P:metabolic pr
	MenE	c32537_g1_i1	0	0	1.747	2977	10	0	86.60%	2	P:metabolic pro
		c810_g1_i1	0	2.554	4.561	465	10	1.10E-58	77.50%	2	P:metabolic pro
		c47809_g1_i1	0.338	0.374	5.469	502	10	5.47E-87	86.70%	2	P:metabolic pro
		c25763_g1_i1	8.175	17.026	12.376	2041	10	0	86.70%	2	P:metabolic pro
		c31684_g1_i1	4.97	22.633	19.871	4137	10	0	84.70%	2	P:metabolic pro
		c32537_g1_i3	9.574	17.971	21.078	2885	10	0	86.60%	2	P:metabolic pro
		c22993_g1_i1	88.781	76.764	71.997	2207	10	0	89.70%	4	P:butyrate metal
		c22627_g1_i1	1028.129	182.702	156.65	1990	10	0	87.20%	11	F:oxalate-CoA l
	MenB	c33824_g1_i1	5.173	596.952	420.248	1388	10	2.05E-178	85.00%	2	F:1,4-dihydrox
		c26824_g1_i1	1.361	28.914	10.27	500	10	9.30E-42	87.70%	4	C:peroxisome;
	DXPS1	c29996_g1_i1	7.962	164.024	148.766	2986	10	0	89.70%	2	F:1-deoxy-D-x
		c29282_g2_i1	0.106	53.363	36.039	1205	10	0	85.30%	2	F:1-deoxy-D-x
		c29282_g1_i1	0	47.144	39.312	1235	10	0	86.70%	2	F:1-deoxy-D-x
		c29855_g1_i2	8.696	10.174	8.882	2551	10	0	78.70%	2	F:1-deoxy-D-x
		c29855_g1_i1	0.811	1.796	3.723	2334	10	0	82.50%	2	F:1-deoxy-D-x
		c38641_g1_i1	1.438	1.755	1.587	265	10	3.41E-44	91.10%	4	F:1-deoxy-D-x
		c30018_g3_i2	0.782	1.287	1.886	1723	10	1.07E-114	96.10%	4	F:1-deoxy-D-x
		c30018_g1_i1	8.155	6.302	11.038	1788	10	0	93.20%	7	F:metal ion bir
		c30018_g3_i3	7.953	4.371	5.888	1411	10	4.93E-163	96.80%	4	F:1-deoxy-D-x
	DXR	c33486_g7_i1	123.834	179.172	144.065	1019	10	4.28E-139	86.40%	6	F:1-deoxy-D-x
		c33486_g1_i5	21.532	13.808	9.571	628	10	4.52E-17	94.00%	28	P:aromatic am
		c33486_g1_i3	0.849	2.741	2.056	753	10	6.93E-17	94.00%	28	P:aromatic am
	ISPD	c23841_g1_i1	25.286	26.297	17.545	1491	10	5.31E-154	88.60%	2	F:2-C-methyl-l
	CDPMEK	c28782_g1_i1	13.357	50.01	33.873	1928	10	0	78.20%	7	P:isopentenyl (
	ISPF	c17510_g1_i1	103.229	174.708	155.632	1119	10	7.35E-115	89.10%	3	F:2-C-methyl-l
	HDS	c23444_g2_i1	80.684	255.5	217.529	2902	10	0	93.30%	7	P:oxidation-re
	HDR	c17511_g1_i1	82.981	278.724	185.972	2392	10	0	88.60%	5	F:4-hydroxy-3
		c5100_g1_i1	6.042	5.399	5.19	1512	10	1.03E-167	74.20%	2	C:chloroplast;
Chlorogenic acid	HQT	c17064_g1_i1	12.025	93.739	33.364	2015	10	0	93.10%	2	F:shikimate O-
	CYP98A35 / C3H1	c24241_g1_i1	2.741	83.928	29.392	957	10	8.28E-154	95.10%	4	F:heme binding;
		c24241_g2_i1	4.951	116.257	53.833	998	10	1.22E-164	93.60%	13	F:identical prote
		c26370_g1_i1	36.703	235.141	117.507	1890	10	0	89.60%	11	F:5-O-(4-couma

		-
		-
		-
		-
		-
		-
		-
		-
		-
		-
		-
		-
		-
		EC:5.4.4.2
		EC:4.2.3.5
		EC:4.2.3.5
		-
		-
		EC:6.2.1.26
		EC:6.2.1.26
		EC:6.2.1.26
		EC:6.2.1.26
		EC:6.2.1.26
		EC:6.2.1.26
		EC:6.2.1.26
		EC:6.2.1.12; EC:6.2.1.26; EC:6.2.1.8
		EC:4.1.3.36
		EC:3.1.2.20; EC:3.1.2
		EC:2.2.1.7
		EC:2.2.1.7
		EC:2.2.1.7
		EC:2.2.1.7
		EC:2.2.1.7
		EC:2.2.1.7
		EC:2.2.1.7
		EC:2.2.1.7
		EC:1.1.1.267
		EC:1.1.1.267
		EC:1.1.1.267
		EC:2.7.7.60
		EC:2.7.1.148
		EC:4.6.1.12
		EC:1.17.7.1
		EC:1.17.7.1; EC:1.17.1.2
		-
		EC:2.3.1.133
		EC:1.14.13.36
		EC:1.14.13.36; EC:1.14.13.21
		EC:1.14.13.36

	Quinate-HCT	c23775_g2_i1	0	7.485	0.16	906	10	4.57E-66	68.10%	1	F:transferase activity, transferring acyl groups other than amino-acyl groups
		c23775_g1_i1	0	10.278	0.719	507	10	5.74E-31	62.00%	1	F:transferase a
		c22655_g1_i1	0	0.81	1.547	339	10	2.48E-26	73.60%	3	P:biosynthetic
		c15374_g1_i2	0.212	8.295	5.359	1693	10	6.53E-142	61.50%	1	F:N-acyltransf
		c7976_g1_i1	1.245	12.988	8.004	1706	10	2.57E-90	73.20%	2	F:N-acyltransf
		c15374_g1_i1	0	28	19.801	1713	10	8.22E-142	61.50%	1	F:N-acyltransf
		c30394_g3_i1	0	56.416	21.268	1728	10	0	71.10%	1	F:transferase a
		c23181_g1_i1	0	259.051	110.002	1640	10	0	74.90%	1	F:transferase activity, transferring acyl groups other than amino-acyl groups
	CCoAOMT1 Caffeoyl-CoA	c20243_g1_i2	0.212	0.914	2.266	690	10	4.54E-90	80.40%	14	P:seed develop
		c25259_g1_i3	0.782	2.834	5.419	294	10	3.26E-43	82.20%	3	F:caffeoyl-Co
		c25259_g1_i1	1.264	5.274	6.787	875	10	4.32E-121	86.80%	3	F:caffeoyl-Co
		c39211_g1_i1	6.553	209.705	175.682	1120	10	9.84E-97	76.40%	3	C:cytosol; P:m
		c41891_g1_i1	100.266	516.949	156.67	1183	10	1.52E-159	95.60%	4	F:caffeoyl-Co
		c32955_g1_i2	2.857	1.256	1.377	1833	10	3.54E-91	94.70%	5	F:caffeoyl-Co
Housekeeping gene	Beta tubulin	c29474_g4_i1	501.311	239.979	231.611	1958	10	0	96.00%	13	C:vacuolar me
	Ubiquitin	c32470_g2_i1	28.365	1.692	1.507	583	10	1.18E-25	99.40%	4	C:plasma memb
		c32470_g2_i4	18.694	1.848	1.896	726	10	6.77E-71	100.00%	4	C:plasma memb
		c31827_g1_i1	20.673	11.015	11.966	1618	10	5.19E-96	98.30%	2	F:acid-amino ac
		c13011_g1_i1	96.975	45.078	48.973	627	10	6.14E-52	96.60%	5	F:protein tag; P:
		c32470_g2_i3	102.447	60.641	64.103	854	10	2.05E-106	99.50%	4	C:plasma memb